ELSEVIER

Contents lists available at ScienceDirect

Science of the Total Environment

journal homepage: www.elsevier.com/locate/scitotenv





Marsh sediments chronically exposed to nitrogen enrichment contain degraded organic matter that is less vulnerable to decomposition via nitrate reduction

Ashley N. Bulseco ^{a,d}, Anna E. Murphy ^{a,e}, Anne E. Giblin ^b, Jane Tucker ^b, Jonathan Sanderman ^c, Jennifer L. Bowen ^{a,*}

- ^a Marine Science Center, Northeastern University, Nahant, MA, USA
- ^b The Ecosystems Center, Marine Biological Laboratory, Woods Hole, MA, USA
- ^c Woodwell Climate Research Center, Falmouth, MA, USA
- ^d Department of Biological Sciences, University of New Hampshire, Durham, NH, USA
- ^e INSPIRE Environmental, Newport, RI, USA

HIGHLIGHTS

- Long-term consequences of N enrichment on carbon storage remains unclear
- Experimental N addition increases respiration but least when chronically enriched
- The active microbial community shifts in response to experimental nitrate exposure
- Chronically enriched marsh sediments have the highest DNF:DNRA ratios
- Chronic nitrogen exposure may lead to less biologically available organic matter

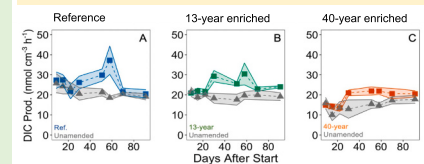
G R A P H I C A L A B S T R A C T

How does chronic nitrogen exposure impact carbon storage in salt marshes?

Salt marshes continue to face nitrogen enrichment and it is unclear what this means for their ability to store carbon.

In flow through reactors, we experimentally enriched sediments with NO₃⁻ collected from:

A relatively pristine marsh
 A marsh enriched to ~70 μmol L¹ NO₃ for 13 years
 A marsh enriched between 100-1000 μmol L¹ for 40 years from wastewater treatment effluent



Experimental NO_3 - enrichment shifted the active microbial community and increased microbial respiration across all sites, but the effect was lowest in the

These results suggest that chronic exposure to elevated nitrogen may lead to residual pools of organic matter that are less biologically available for decomposition.

ARTICLE INFO

Editor: Elena Paoletti

Keywords: Nutrient enrichment Denitrification DNRA Sulfate reduction Carbon storage Decomposition Microbes

$A\ B\ S\ T\ R\ A\ C\ T$

Blue carbon habitats, including salt marshes, can sequester carbon at rates that are an order of magnitude greater than terrestrial forests. This ecosystem service may be under threat from nitrate (NO $_3$) enrichment, which can shift the microbial community and stimulate decomposition of organic matter. Despite efforts to mitigate nitrogen loading, salt marshes continue to experience chronic NO_3 enrichment, however, the long-term consequence of this enrichment on carbon storage remains unclear. To investigate the effect of chronic NO_3 exposure on salt marsh organic matter decomposition, we collected sediments from three sites across a range of prior NO_3 exposure: a relatively pristine marsh, a marsh enriched to \sim 70 μ mol L^{-1} NO_3 in the flooding seawater for 13 years, and a marsh enriched between 100 and 1000 μ mol L^{-1} for 40 years from wastewater treatment effluent. We collected sediments from 20 to 25 cm depth and determined that sediments from the most chronically enriched site had less bioavailable organic matter and a distinct assemblage of active microbial taxa compared to the other two sites. We also performed a controlled anaerobic decomposition experiment to test whether the

E-mail address: je.bowen@northeastern.edu (J.L. Bowen).

^{*} Corresponding author.

legacy of NO_3^- exposure influenced the functional response to additional NO_3^- . We found significant changes to microbial community composition resulting from experimental NO_3^- addition. Experimental NO_3^- addition also increased microbial respiration in sediments collected from all sites. However, sediments from the most chronically enriched site exhibited the smallest increase, the lowest rates of total NO_3^- reduction by dissimilatory nitrate reduction to ammonium (DNRA), and the highest DNF:DNRA ratios. Our results suggest that chronic exposure to elevated NO_3^- may lead to residual pools of organic matter that are less biologically available for decomposition. Thus, it is important to consider the legacy of nutrient exposure when examining the carbon cycle of salt marsh sediments.

1. Introduction

Salt marshes store carbon at rates that are orders of magnitude greater than terrestrial forests due to large inputs of organic matter (OM) from primary production coupled with slow decomposition rates. The extent to which salt marshes store carbon depends largely on the balance between inputs from primary production and sedimentation and losses from decomposition, with the latter ultimately determining how much carbon is buried over long time-scales (Burdige, 2007; Spivak et al., 2019). While several studies document decomposition rates in response to shifting environmental conditions, such as temperature (Kirschbaum, 1995; Kirschbaum et al., 2011; Conant et al., 2011; Lehmann and Kleber, 2015; Smith et al., 2022) and sea level rise (Kirwan et al., 2013; Wang et al., 2019), there is uncertainty about the effect added nitrogen (N) has on the balance between primary production and decomposition and, in particular, about the form of nitrogen in question (Bulseco et al., 2019; Bowen et al., 2020).

Tremendous efforts to mitigate consequences of increased N loading from sewage, urban and agricultural runoff, and atmospheric N deposition (Galloway et al., 2008; Lloret and Valiela, 2016; Galloway et al., 2017) decreased eutrophication in some regions (Zedler, 2000; Warren et al., 2002); however, many salt marshes worldwide continue to experience chronic nutrient enrichment (Bricker et al., 2008; Crosby et al., 2021) with uncertain consequences for carbon storage. Increased N loading can alleviate N limitation and promote primary production (Valiela et al., 1975; Morris, 1991; Langley et al., 2013; Morris et al., 2013). N in the form of nitrate (NO₃), however, can also serve as an electron acceptor in heterotrophic microbial metabolisms and thus lead to increased respiration of OM (Wigand et al., 2009; Watson et al., 2014; Martin et al., 2018; Bowen et al., 2020) and decreased sediment stability (Turner, 2011; Deegan et al., 2012; Mueller et al., 2018). Further, because NO₃ respiration yields more energy than other anaerobic metabolisms, such as sulfate reduction, there is a "NO3-accessible" pool of OM that can be respired only under high NO₃ availability (Bulseco et al., 2019). What remains unclear, however, is whether a legacy of NO₃ enrichment can diminish that NO₃-accessible pool of OM, thereby fundamentally increasing the stability of the long-term marsh carbon pool.

Increased N concentrations may stimulate a microbial response, causing a shift in overall metabolic capacity that affects the amount of decomposed OM. Nutrient enrichment to salt marshes alters the active microbial community (Kearns et al., 2016) though it does not seem to increase bacterial production (Bowen et al., 2009). The community structure of denitrifying microbes can also shift (Bowen et al., 2013; Graves et al., 2016; Angell et al., 2018) and nutrient enrichment can increase both the diversity and abundance of putative fungal denitrifiers (Kearns et al., 2019), potentially translating to more OM oxidation compared to systems without exogenous sources of NO₃. Exogenous N can select for N-adapted microbes that produce more extracellular enzymes to help oxidize complex OM (Treseder et al., 2011) and may influence the metabolic strategies used by the microbial community. For example, increased N supply may shift the relative proportion of dissimilatory nitrate reduction to ammonium (DNRA) to denitrification (DNF) (Koop-Jakobsen and Giblin, 2010). The ratio of these two pathways is ecologically important because DNF results in N loss while DNRA conserves N in the ecosystem (Burgin and Hamilton, 2007). High NO_3^- conditions appear to favor DNF, whereas NO_3^- limitation concurrent with biologically available OM favors DNRA (Burgin and Hamilton, 2007; Algar and Vallino, 2014; Hardison et al., 2015) and both processes appear to be mediated by plant species composition (Ledford et al., 2020). Understanding how the microbial community changes in response to increased N supply, whether chronic nutrient enrichment leaves behind a legacy of effects, and how these legacies influence future OM decomposition, is critical to better understand long term carbon storage in salt marsh systems.

Our objective was to examine salt marsh sediments from sites exposed to a range of NO₃ concentrations, varying both in magnitude (below detection to up to 1000 μ mol L⁻¹) and duration (no exposure to 40 years of chronic enrichment), by characterizing OM quality and the associated microbial community. We collected sediments from below the rooting zone, so inputs of new organic matter from plant rhizodeposits would be minimized. We hypothesized that sediments from sites with greater NO3 enrichment would exhibit lower OM quality and harbor microbes better adapted to a high N environment. To examine if these site differences influenced the functional response to an additional supply of NO₃, we performed a controlled flow through experiment under anoxic conditions, where we added 500 $\mu mol~L^{-1}~NO_3^-$ to each sediment type and measured the metabolic response and changes to the microbial community compared with unamended controls. We hypothesized that 1) NO₃ addition would stimulate sediment microbial respiration due to the presence of an energetically favorable electron acceptor, 2) this stimulation would be less pronounced in chronically enriched sediments due to a less biologically available OM pool, and 3) NO₃ addition would alter the active microbial community to a lesser extent in sediments collected from chronically enriched sites due to the presence of taxa already conditioned to survive in a high N environment.

2. Methods

2.1. Sample collection

We collected sediment cores (5 cm diameter, 30 cm deep) ~ 1 m from the creek bank from the tall ecotype of Spartina alterniflora in three salt marshes varying in time and intensity of prior NO₃ exposure located in the Great Marsh in Northeastern Massachusetts, USA, the study location of the Plum Island Ecosystem Long-Term Ecological Research (LTER) site (Fig. S1). Our study sites included (1) West Creek (hereby "reference"), a relatively pristine reference marsh, (2) Sweeney Creek ("13-year enriched"), which was experimentally enriched with 70 μM NO₃ dissolved into flooding tide waters for 13 years as part of the TIDE project (Deegan et al., 2007; Deegan et al., 2012), and (3) Greenwood Creek ("40-year enriched"), which has received UV-sterilized wastewater effluent from a nearby wastewater treatment plant for 40 years, with NO_3^- and ammonium (NH₄) concentrations reaching 1000 μ M and 100 µM, respectively (Graves et al., 2016). Prior to being experimentally enriched, the 13-year enriched marsh was unaffected by nutrient loading (Deegan et al., 2007). All sites are within 10 km of each other with similar climate and are flooded twice daily with tidal ranges between 2.6 and 4 m (Deegan et al., 2007; Graves et al., 2016). We selected these sites due to their close proximity and similarity in characteristics with the exception of nitrogen legacy, which would allow us to test our hypotheses.

To focus on legacy effects that occur within deeper sediments where C storage occurs (Chmura et al., 2003) and to minimize the influence of plant rhizodeposits as much as possible, we sectioned and homogenized four cores from each site at 20–25 cm depth. To characterize samples collected in situ, we froze a subsample of sediment at $-20~^{\circ}\text{C}$ for OM characterization, and immediately flash froze additional subsamples, which were stored at $-80~^{\circ}\text{C}$ for nucleic acid extraction; we then used the remaining sediment for the decomposition experiment (See Section 2.2). We define "site" as the location from which the sediments were collected; in our decomposition experiment using these site-specific sediments, we have two treatments - a NO_3^- addition and an unamended control.

2.2. Decomposition experiment

We conducted a flow through reactor (FTR) experiment using sediments collected from each site to assess how decomposition rates would respond to further NO_3^- addition. Our FTR experimental system (Bulseco et al., 2019) is a modified version of a previously described system (Pallud and Van Cappellen, 2006; Pallud et al., 2007) that provides biogeochemical rates under steady-state in isolation from other environmental conditions that may obscure measurements in the field (e.g., the influence of plant communities or tidal flux). Each FTR consists of two polyvinyl chloride, radially scored caps that ensure uniform flow and are sealed with O-rings to prevent leakage. To assess flow characteristics in the reactors, we performed breakthrough experiments using a conservative tracer, bromide (Table S1).

Under anoxic conditions, maintained in an anerobic chamber and monitored using a luminescent dissolved oxygen probe (Hach LDO101), we loaded the FTRs with homogenized sediment collected from 20 to 25 cm at each site. Reactors were randomly assigned to a treatment, either plus- NO_3^- (500 μ mol L⁻¹ NO_3^- in 0.2 μ m filtered seawater) or unamended (0.2 µm filtered seawater only, representing natural marsh conditions). Seawater for the reservoirs that flow into the FTR was collected from Woods Hole, MA, filtered (0.2 µm pore size), and sparged with N2 gas until reaching anoxia. We then spiked the plus-NO3 reservoir with K¹⁵NO₃ (Cambridge Isotope Laboratories, Andover, MA, USA). Reactors from each site received water from their reservoir at a flow rate of 0.08 $mL min^{-1}$ under continuously anoxic conditions (n = 4 for each site x treatment combination). After 10 days, the reactors reached steady state and we collected water samples approximately every 10 days for 100 days, from both the reservoirs and effluents to measure total microbial respiration (dissolved inorganic carbon; DIC), ammonium (NH₄⁺) and sulfide (HS⁻) production, and NO₃ consumption. We also estimated SO₄² reduction from measurements of dissolved HS⁻ loss and changes in the total sulfur (S) pool of the sediment. To determine partitioning among NO₃ reduction pathways in the plus-NO₃ treatment, we followed the fate of the ¹⁵N tracer into various end products (^{29,30}N₂ and ¹⁵NH₄⁺). To assess changes in the bulk sediment and in the microbial community, we homogenized sediment from each FTR at the end of the experiment and immediately sub-sampled sediments for nucleic acid extraction and organic matter analysis.

2.3. Biogeochemical analyses in the flow through water

We collected water samples approximately every 10 days from both the plus- NO_3^- and unamended treatment effluent, as well as from each reservoir, to quantify biogeochemical processes resulting from microbial activity in the decomposition experiment. We measured DIC as an indicator of total microbial respiration on an Apollo SciTech AS-C3 DIC analyzer and NO_3^- on a Teledyne T200 NOx analyzer using chemiluminescence (Cox, 1980). We measured NH_4^+ and HS^- colorimetrically on a Shimadzu 1601 spectrophotometer following standard protocols (Solorzano, 1969; Gilboa-Garber, 1971). To quantify analyte

consumption or production rate over time, we used the following equation (Pallud and Van Cappellen, 2006):

$$R = \frac{(C_{out} - C_{in}) \times Q}{V} \tag{1}$$

where R is the consumption or production rate of interest, C_{out} and C_{in} are the effluent and reservoir analyte concentrations, respectively, Q is the measured flow rate in L hour $^{-1}$, and V is the FTR volume (31.81 cm $^{-3}$). We calculated a cumulative flux for each analyte by integrating between each measured point throughout the experiment. Since background SO_4^{2-} concentrations are typically high in seawater (\sim 28 mmol L^{-1}), we determined SO_4^{2-} reduction rates (SRR) by calculating the sum of the total production of HS $^-$ and total sulfur (S) at the end of the experiment.

To determine the relative contribution of $^{15}NO_3^-$ reduction pathways, we measured dissolved N_2 using a membrane inlet mass spectrometer (Kana et al., 1994) with a 500 °C inline furnace and copper column to remove oxygen (Eyre et al., 2002; Lunstrum and Aoki, 2016). We considered denitrification as the production of $^{29}N_2$ and $^{30}N_2$ from added $^{15}NO_3^-$ tracer and calculated rates as follows (Nielsen, 1992):

$$D_{15} = p29 + 2p30 \tag{2}$$

where D_{15} is denitrification from $^{15}NO_3^-$ and p29 and p30 is production of $^{29}N_2$ and $^{30}N_2$, respectively. We only added NO_3^- as $^{15}NO_3^-$, ambient concentrations of $^{14}NO_3^-$ were below detection, and production of $^{14}NO_3^-$ from nitrification should be negligible because our experiment was conducted under anoxic conditions. As a result, we did not calculate D_{14} and we considered $^{29}N_2$ as indicative of anammox. We followed the OX/MIMS method, which uses hypobromite to oxidize NH_4^+ to N_2 , to measure DNRA (Yin et al., 2014) and calculated DNRA rates as:

$$DNRA_{15} = p29 + 2p30 (3)$$

where DNRA₁₅ is DNRA from ¹⁵NH₄⁺ and p29 and p30 represent production of ²⁹N₂ and ³⁰N₂ from oxidized ¹⁵NH₄⁺, respectively. We did not make these measurements in the unamended treatment, as there was no added ¹⁵NO₃⁻. Isotope tracer measurements were completed at 8, 11, and 12-weeks after the start of the experiment, with no DNRA measurements available on week 11 due to limited sample volume.

2.4. Sediment organic matter analyses

We performed elemental analysis (% organic C and % total N) on sediments collected from each site both before, and at the end of the decomposition experiment, using a Costech Elemental Analyzer 4010. Sediments were dried at 65 °C and fumed with 12 N hydrochloric acid. We used the same dried samples to measure % sulfur (S) by combusting them at 1350 °C and measuring sulfur dioxide production on a LECO S635 S Analyzer. We dried additional samples at 105 °C to calculate bulk density and further combusted those samples at 550 °C for three hours to obtain %OM as loss-on-ignition (LOI).

We used Fourier Transform-Infrared Spectroscopy (FT-IR) to examine differences in bulk OM across sites in more detail. This spectroscopic technique provides detailed information about the relative abundance of chemical functional groups, thereby allowing for inferences about OM properties, such as the degree of decomposability. We ran finely ground sediment dried at 40 °C for 48 h on a Bruker Vertex 70 FT-IR with a Pike AutoDiff diffuse reflectance accessory. To obtain data, we collected scans at a 2 cm⁻¹ resolution in the mid-IR range (4000–400 cm⁻¹) as pseudo-absorbance (log[1/reflectance]) in diffuse reflectance mode. We used 60 co-added scans per spectrum using a mirror for background correction. To baseline correct the data, we transformed each raw spectrum using a calculated two-point linear tangential baseline in Unscrambler X and assigned peaks (Table S2) corresponding to aromatic carbon and carboxyl groups (Parikh et al., 2014; Margenot et al., 2015). We calculated the ratio between these two

groups to determine a 'degradation index', with higher ratios indicating that the sediment OM was more resistant to degradation (Ding et al., 2002; Veum et al., 2013).

2.5. Sediment nucleic acid extraction, amplification, and sequencing

To assess differences in the in situ active microbial communities among our sites and as a result of our decomposition experiment, we extracted RNA using a method modified from Mettel et al. (2010) according to Kearns et al. (2016). While DNA provides information on the total microbial community, it cannot distinguish among inactive and actively metabolizing cells; therefore, we chose to focus on RNA, which we can use to assess the portion of the microbial community contributing to measured ecosystem processes. We checked for DNA contamination in the RNA using general bacterial primers 515F and 806R (Bates et al., 2011), and removed contamination using DNase I (New England BioLabs, Ipswich, MA, USA). Lastly, we reverse transcribed 2 μ L RNA to cDNA using random hexamer primers and an Invitrogen Superscript III cDNA synthesis kit for RT-PCR (Life Technologies, Carlsbad, CA, USA).

After confirming the presence of cDNA using SYBR Safe gel electrophoresis (Thermo Fisher Scientific, Waltham, MA, USA), we amplified in triplicate the V4 region of the reverse transcribed 16S rRNA using the general bacterial primers (Bates et al., 2011) (515F; 5'-GTGCCAGCMGCCGCGGTAA-3') and 806R (5'-GACTACHVGGGTWTC-TAAT-3') with Illumina adaptors (Caporaso et al., 2012) and individual 12-bp GoLay barcodes on the reverse primer, using 5-Prime Hot Master Mix in a PCR reaction, with cycling conditions recommended by the Earth Microbiome Project (Caporaso et al., 2011). We size selected by gel excision, gel purified PCR products using a Qiagen® QIAquick gel purification kit and quantified the products using a Qubit® 3.0 fluorometer. After pooling to equimolar amounts, we performed sequencing on an Illumina MiSeq platform using the paired-end 250 bp 500 cycle kit with V2 chemistry at University of Massachusetts Boston. All reads are deposited in the NCBI Sequence Read Archive under BioProject ID PRJNA1014411.

We demultiplexed and analyzed 16S rRNA sequence data using QIIME 2, version 2019.10 (Caporaso et al., 2010). Using the DADA2 plugin (Callahan et al., 2016), we inferred amplicon sequence variants (ASVs) with a maxEE of 2 and the consensus chimera removal method. We then assigned taxonomy against the SILVA 132 database (Quast et al., 2012) and removed any sequences matching Archaea, Chloroplasts, and Mitochondria. Following quality filtering, we had a total of 1,040,754 sequences with an average of 28,909 sequences per sample. The sequence data contained a total of 15,204 ASVs, corresponding to a total of 7149 ASVs in the dataset from the in situ samples, and a total of 12,288 ASVs across samples from the decomposition experiment, all of which we imported into the Phyloseq package for downstream statistical analysis (McMurdie and Holmes, 2013; Callahan et al., 2016).

2.6. Statistical analyses

To assess differences in OM characteristics among sites, we performed a one-way ANOVA for variables that met assumptions of normality and equal variances (%N and C:N) and used a Tukey HSD test for variables that were significantly different among sites. For variables that did not meet assumptions of a one-way ANOVA (OM, %C, and %S), we performed a non-parametric Kruskal-Wallis analysis among sites and applied a Dunn test for multiple comparisons. To characterize the active microbial community at each of the sites, we identified the 40 most dominant ASVs across sites, and visualized their relative abundances at the family level using a stacked bar plot.

Following the decomposition experiment, we examined differences in DIC production across treatments and sites and performed repeated measures ANOVA using days after start as a random factor. We compared cumulative rates of DIC production, and NO_3^- and SO_4^{2-} reduction (HS $^-$ production + S storage), across treatments and sites

using a two-way ANOVA with a Tukey HSD test for multiple comparisons and calculated effect sizes to measure the magnitude of response to NO_3^- addition. To further explore the influence of initial bulk C supply on DIC production, we calculated total C loss by taking the proportion of C released as DIC divided by the total mass of C per reactor using sediment bulk density and %C. We calculated the proportion of DIC generated from SO_4^{2-} and total NO_3^- reduction, and DNF and DNRA more specifically in the plus- NO_3^- treatment, using stoichiometry. We also performed a one-way ANOVA comparing DNF, DNRA, and anammox across sites, and calculated the percentage of each process contributing to total NRR. Finally, we determined DNF:DNRA ratios to assess the contribution of DNRA relative to DNF and compared this ratio across sites using a one-way ANOVA.

To examine changes in OM characteristics (OM, %C, %N, C:N, and %S) that occurred during the FTR experiment, we used a two-way ANOVA with an interaction between 'Treatment' and 'Site' and proceeded with an additive model with a Tukey HSD test if the interaction effect was insignificant. We performed a principal coordinate analysis (PCoA) across the mid-IR spectra (4000–400 cm⁻¹) and tested for differences among treatment and site using a PERMANOVA with 999 permutations on a resemblance matrix constructed using Manhattan distance. To better understand which spectral bands and associated functional groups were responsible for observed patterns in the PCoA, we plotted Pearson's correlation coefficients against wavenumber, with peaks exhibiting the greatest absolute change that most influenced the PCoA. We then performed a linear regression between DIC production and degradation index values across all treatments and sites.

To assess shifts in the active community, we calculated Bray-Curtis similarity values on the ASVs from the 16S rRNA sequences. We visualized these differences using non-metric multidimensional scaling using the ordinate command in Phyloseq. We tested for differences across sites and by treatment using adonis and tested for the dispersion of our centroids using betadisper. We used the DESeq2 negative binomial Wald test with Benjamini-Hochberg false discovery rate control to identify active microbial taxa that were differentially abundant between the plus-NO $_3^-$ and unamended treatments (Love et al., 2014). To account for potential differences among sites, we ran the analysis for the reference, 13-year, and 40-year enriched sites separately and visualized all ASVs that were significantly different (p-adj < 0.05) in a heatmap constructed with Anvi'o, version 6.1 (Eren et al., 2015) clustered by Bray-Curtis dissimilarity.

3. Results

3.1. Initial site characterization

There were no significant differences in %OM, %C, % N or molar C:N of initial sediments across sites (Table 1); however %S was greater in the reference site compared to the 40-year enriched site (p=0.01, $X^2=8.14$) and the degradation index (aromatic-to-carboxylic carbon) was highest at the 40-year enriched site compared to both the reference and 13-year enriched sites (Fig. 1A; p<0.001, $F_{2,9}=20.99$). These differences were also evident in the baseline corrected spectra (Fig. 1B), where the 40-year enriched sediments demonstrated polysaccharide depletion (1080 and 1110 cm⁻¹) and enrichment of aromatic compounds (1650 cm⁻¹).

Within the initial sediments, of the 40 active ASVs with the highest relative abundance, the Campylobacteraceae dominated the active communities, representing ~36.4, 28.0, and 18.5 % at the reference, 13-year, and 40-year enriched sites, respectively, (Fig. 2). Twelve ASVs within the Campylobacteraceae family were assigned to the *Arcobacter* genus (Table S3). Oceanospirallilaceae was the second most dominant active family across all sites, representing ~9.5 % at the reference site, 12.6 % at the 13-year, and 14.0 % at the 40-year enriched site. Two of these ASVs were assigned to the genus *Amphritea*, and two others were assigned to *Marinobacterium* and *Marinomonas*. The families

Table 1 Average \pm SD bulk density (BD), % organic matter (OM), % carbon, % nitrogen, molar C:N, and % sulfur (N = 4) prior to (in situ) and at the end of the decomposition experiment for each treatment ("Unamended" versus "Plus-NO $_3$ ") in sediments from the three different sites (Reference, 13-year, and 40-year enriched). Different letters indicate significant differences (α = 0.05). Salinity Data from Deegan et al. (2007) and Giblin & Forbrich, Unpublished data.

	Salinity	BD	% OM	% Carbon	% Nitrogen	Molar C:N	% Sulfur
In situ							
Reference	$20.8 (0.8)^{\gamma}$	NA	20.01 (0.91)	5.09 (0.23)	0.54 (0.06)	11.12 (1.28)	$1.42 (0.26)^{a}$
13-year	$24.0 (0.8)^{\gamma}$	NA	21.39 (0.69)	5.51 (0.23)	0.61 (0.08)	10.50 (0.97)	0.84 (0.44) ^{ab}
40-year	$8.4-19.1^{\Psi}$	NA	26.80 (8.10)	6.90 (1.56)	0.60 (0.06)	11.90 (1.61)	0.48 (0.07) ^b
Decomp. Exp. Unamended							
Reference	NA	0.55 (0.01)	19.08 (0.92) ^a	$5.22(0.04)^{a}$	$0.60 (0.06)^a$	$10.20 (1.05)^{a}$	$1.37 (0.19)^a$
13-year	NA	0.53 (0.02)	$20.98 (0.72)^a$	$5.65 (0.39)^a$	0.61 (0.09) ^{ab}	10.86 (1.36) ^a	$0.83 (0.32)^{b}$
40-year	NA	0.51 (0.06)	26.41 (7.14) ^b	6.92 (1.56) ^b	0.71 (0.09) ^b	11.27 (2.04) ^b	$0.58 (0.03)^{c}$
Plus-NO ₃							
Reference	NA	0.58 (0.01)	18.84 (0.49) ^a	4.89 (0.12) ^a	$0.52 (0.06)^a$	11.00 (1.17) ^a	1.46 (0.15) ^a
13-year	NA	0.56 (0.02)	20.94 (1.40) ^a	5.85 (0.56) ^a	0.64 (0.08) ^{ab}	10.73 (1.48) ^a	0.76 (0.34) ^b
40-year	NA	0.52 (0.06)	27.09 (6.67) ^b	6.78 (1.48) ^b	0.60 (0.07) ^b	12.96 (1.45) ^b	0.50 (0.8) ^c

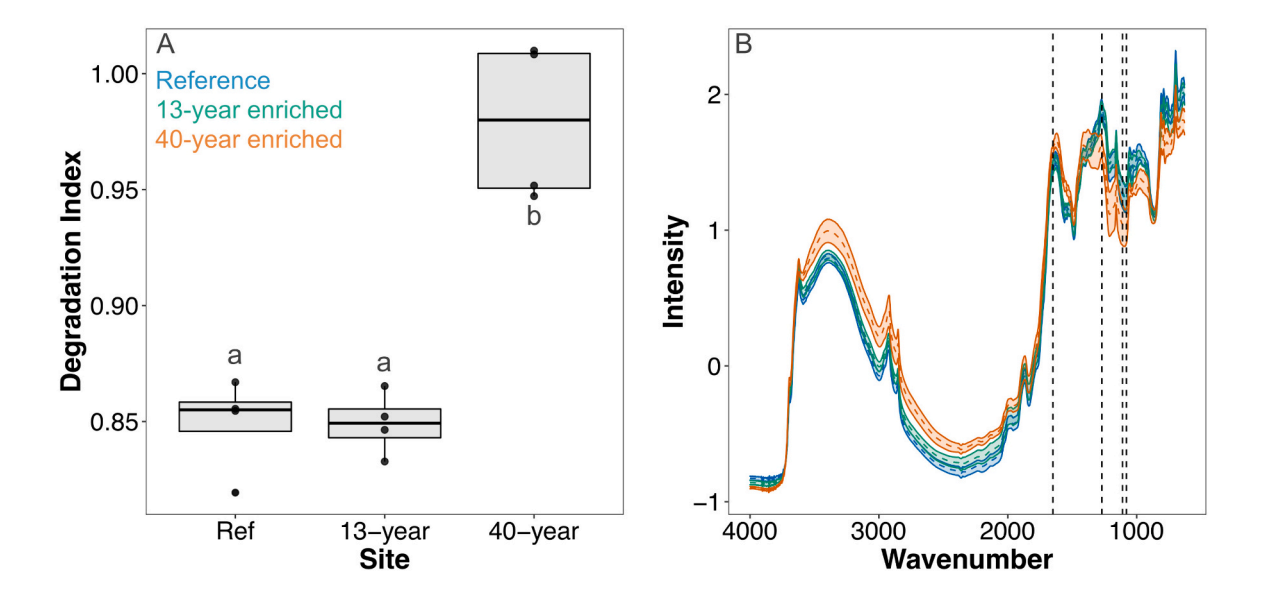


Fig. 1. Organic matter (OM) quality at each site before the start of the decomposition experiment as assessed with Fourier Transform-Infrared Spectroscopy (FT-IR). (A) Boxplot of the degradation index, calculated as the ratio between aromatic carbon and carboxylic carbon, across sites. Black dots represent values for each individual reactor (n = 4), and different letters indicate significant differences between groups according to a Tukey HSD test. (B) Baseline corrected mean mid-IR spectra \pm SE of each site before the start of the experiment. Dashed vertical lines indicate wavenumbers for aromatic carbon (1650 cm⁻¹) and carboxyl groups (1270 cm⁻¹) used to calculate the degradation index, as well as polysaccharides (1080, 1110 cm⁻¹).

Desulfobacteraceae (genus *Desulfosarcina*) and Helicobacteraceae (genus *Sulfurimonas*), were relatively more important at the reference site, with the latter being completely absent from the 40-year enriched site, while Psychromonadaceae (genus *Psychromonas*), Desulfobulbaceae, and Vibrionaceae (genus *Vibrio*) were relatively more abundant at the 13-year site. In contrast, Oceanospirallaceae, Pseudomonadaceae (genus *Pseudomonas*), Rhodocyclaceae (genus *Denitromonas*), and Shewanellaceae (genus *Shewanella*), and Geobacteraceae (genus geopsychrobacter) were all highest at the 40-year enriched site (Fig. 2; Table S3).

3.2. Microbial respiration

During the decomposition experiment, DIC production was greater in the plus-NO $_3^-$ compared to the unamended treatment, regardless of site ($p=0.002,\ F_{1,20}=12.25$). NO $_3^-$ stimulated the greatest average DIC production in the reference sediments (26.48 \pm 5.51 in the plus-NO $_3^-$ treatment versus 21.67 \pm 2.55 nmol cm $^{-3}$ h $^{-1}$ in the unamended treatment, Fig. 3A) compared to the 13-year (24.57 \pm 3.88 versus 19.41 \pm 0.91 nmol cm $^{-3}$ h $^{-1}$, Fig. 3B) and 40-year enriched sediments (18.57

 \pm 3.70 versus 14.71 \pm 2.53 nmol cm⁻³ h⁻¹, Fig. 3C; p < 0.001, F(2.36) = 18.75). Overall DIC production was lowest in the 40-year enriched sediments, regardless of treatment (Fig. 3D; p < 0.001, $F_{(2,14)} = 48.33$). There was no significant interaction between treatment and site, however, the effect size (Cohen's d) in response to NO₃ addition was 1.65 (reference), 1.90 (13-year), and 0.78 (40-year), corresponding to greater similarity between the unamended and plus-NO₃ treatment from the 40year enriched site than from the reference and 13-year enriched sites. Similarly, NO₃ addition stimulated the greatest proportion of total organic carbon loss in the reference sediments and least in the 40-year enriched sediments (p < 0.001, $F_{2,18} = 30.61$), with the plus-NO₃ treatment demonstrating greater carbon loss when compared to the unamended treatment overall (Fig. 3E; p < 0.001, $F_{1,18} = 17.62$). There were no significant differences by treatment or site in NO₃ reduction rate (Fig. 4A) although the 40-year enriched site was consistently lower over time until the final sampling timepoints. Similarly, the cumulative NO₃ reduction (Fig. 4B) was not significantly different by site but was generally lower for the 40-year enriched site. The ratio of DIC production to NO_3^- reduction was $0.52\pm0.05,\,0.55\pm0.08,\,$ and 0.50 ± 0.07 for

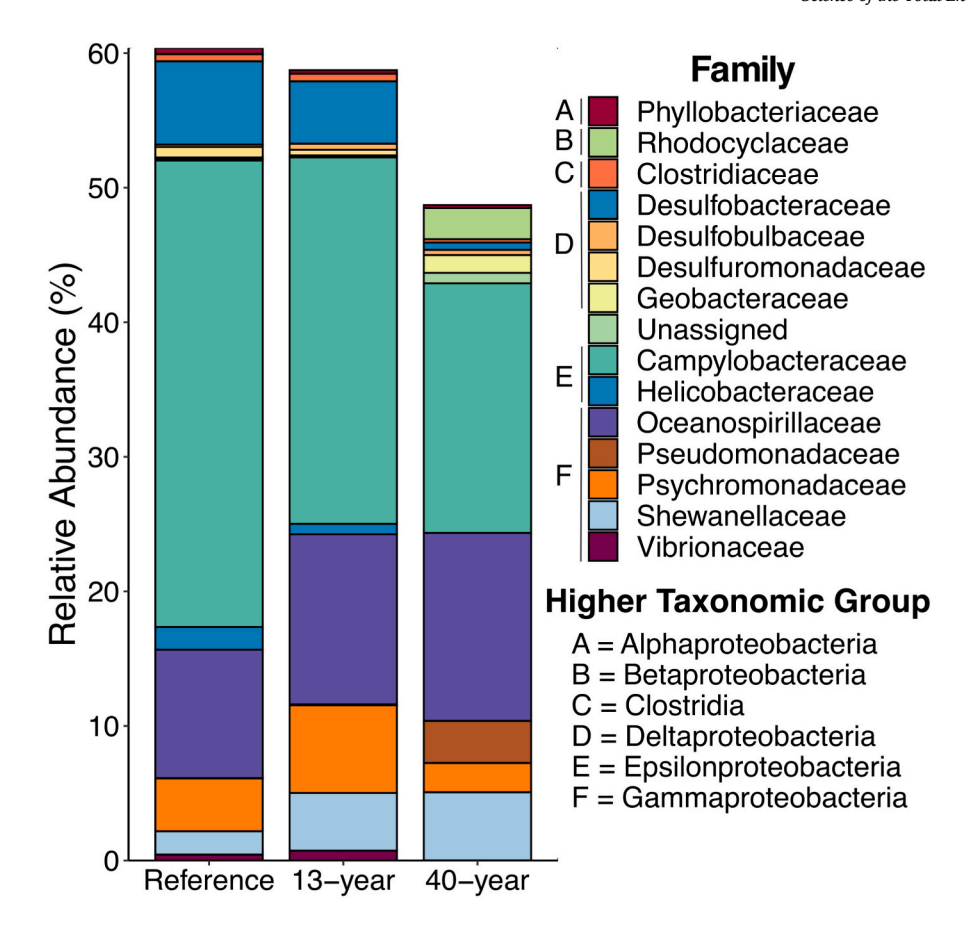


Fig. 2. Top 40 active taxonomic groups with the highest relative abundance in sediment collected at 25 cm from each site prior to the decomposition experiment. Taxa are listed at the family level with letters indicating the relevant class. See Supplemental Table S3 for more taxonomic information and the relative abundances of the individual amplicon sequence variants (ASVs).

the reference, 13-year enriched, and 40-year enriched sites, respectively, which was considerably lower than the ratio of 1.25 (for DNF) or 2.0 (for DNRA) as predicted by stoichiometry. There were no significant differences by treatment or site for sulfide production rate (Fig. 4C) and cumulative sulfate reduction (Fig. 4D), but the reference site trended toward high sulfate reduction overall.

The sum of DNF, DNRA, and anammox accounted for $\sim\!36.5,\ 34.0,\$ and $47.7\$ % of total NO $_3^-$ reduction rate (NRR) on week 8 and $\sim 82.8,\$ 74.4, and 39.3 % of NRR on week 12 at the reference, 13-year, and 40-year enriched sites, respectively (Table 3). Anammox was a minor portion of measured NRR. DNF rates were significantly greater at the 13-year enriched site when compared to the 40-year enriched site ($p=0.02,\ X^2=7.1;\ Table\ 2$), while DNRA rates were significantly lower at the 40-year enriched site ($p=0.005,\ X^2=10.35;\ Table\ 2$) compared to both the reference and 13-year enriched sites. The DNF:DNRA ratios were 3.0 ± 1.6 (Reference), 3.03 ± 1.4 (13-year enriched), and 7.9 ± 6.7 (40-year enriched), indicating that DNF was always the dominant NO $_3^-$ reduction process. The 40-year enriched site, however, exhibited less than half the amount of DNRA relative to DNF when compared to the reference and 13-year enriched site.

3.3. Organic matter characteristics resulting from the decomposition experiment

At the end of the experiment, there were no significant differences in bulk sediment properties by treatment (%OM, %C, %N, molar C:N, and %S). A PCoA of the FT-IR spectra (Fig. 5A), however, showed a significant separation by site along the primary axis (explaining 84.5 % of the

variation (PERMANOVA, p=0.001, pseudo-F_{2,27} = 48.78), but no effect of treatment (p=0.69). Site differences largely resulted from decreased polysaccharides (C—O band at 1080 cm⁻¹) and increased aromatic (C=C band at 1650 cm⁻¹), aliphatic (asymmetric and symmetric stretching vibration C—H bands at 2924 cm⁻¹ and 2850 cm⁻¹, respectively), and amide C (N—H and C=N bands at 1575 cm⁻¹; Fig. 5B) in the 40-year enriched site. DIC production significantly decreased with increasing carbon complexity as indicated by the higher degradation index values (Fig. 5C; p<0.001, $F_{1,10}=26.42$, $R^2=0.70$).

3.4. Microbial community response to decomposition experiments

Differences in the active microbial community that were observed across sites prior to the NO₃ addition (Fig. 2) persisted at the end of the NO₃ addition experiment (Fig. S2). Visualization of Bray-Curtis dissimilarity by nonmetric multidimensional scaling indicates strong site differences in the active microbial community. This is supported by adonis results, which indicate significant differences by site (F = 6.39, p< 0.01) and treatment (F = 2.61, p < 0.01), but no significant interaction. The dispersion of the data around centroids was significantly different across sites (F = 14.35, p < 0.01), with much greater dispersion in the 40-year enriched site, suggesting caution in interpreting adonis results. There were, however, significant differences in relative abundance of ASVs from the active microbial community, resulting in 46 ASVs identified as significantly different between plus-NO3 and unamended treatments across all three sites. The 40-year site had the greatest number ASVs that were significantly different (N = 33), followed by the reference site (N = 13), and the 13-year enriched site (N = 13)

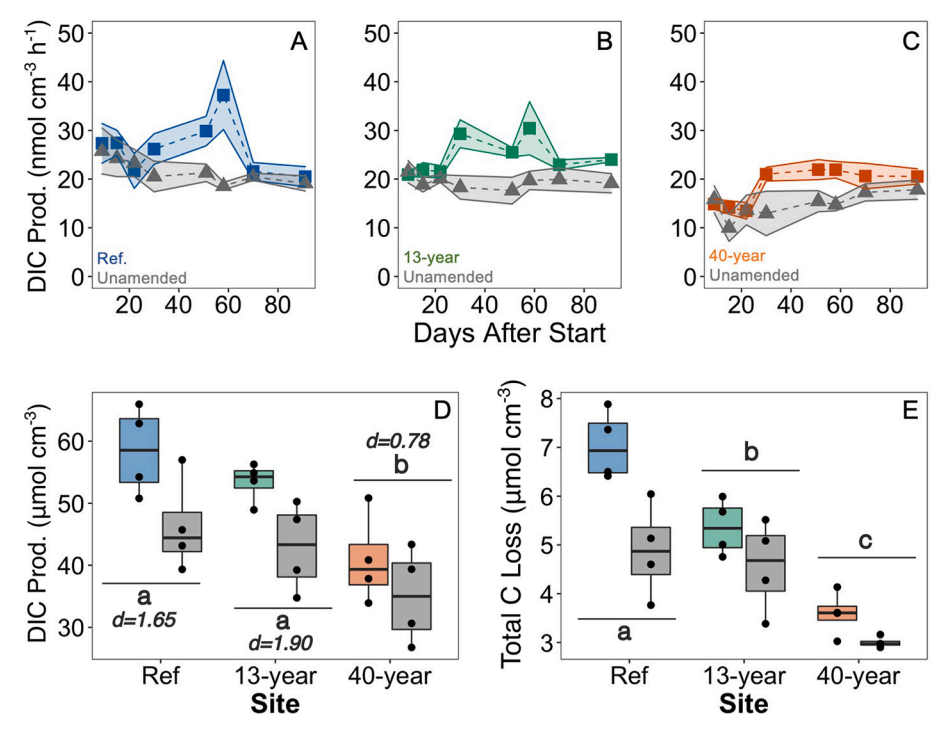


Fig. 3. Average (\pm SE, indicated by shaded region) dissolved inorganic carbon (DIC) production over time (days) for the reference (A), 13-year enriched (B) and 40-year enriched (C) site that correspond to different levels and durations of chronic nitrogen exposure (n = 4). Boxplot of cumulative DIC production with effect size indicated by Cohen's "d" (D) and total carbon (C) loss, calculated as the proportion of C released as DIC divided by the total mass of C per reactor (E) over the course of the decomposition experiment between unamended (gray) and plus-NO $_3^-$ treatments. In each case, the plus-NO $_3^-$ treatment had higher DIC production than the unamended treatment. Different letters indicate significant differences among sites according to a Tukey HSD test.

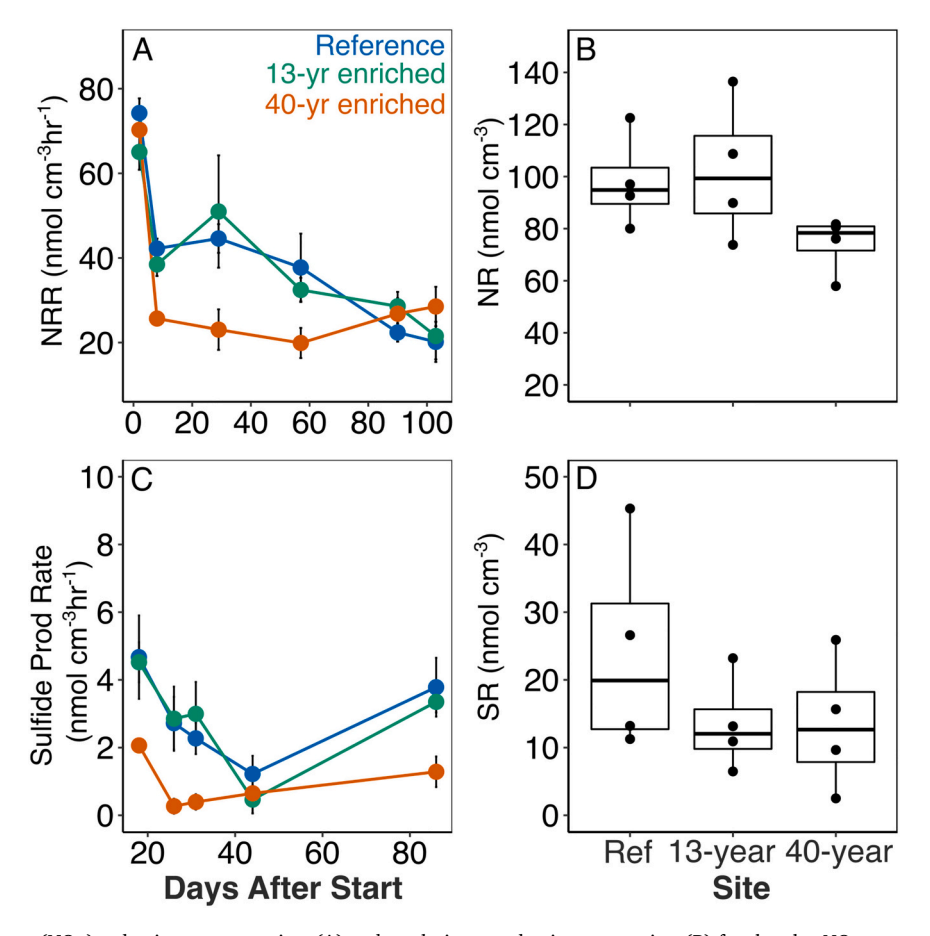


Fig. 4. Average (\pm SE) nitrate (NO $_3^-$) reduction rate over time (A) and total nitrate reduction across sites (B) for the plus-NO $_3^-$ treatment. Average (\pm SE) sulfide production rate over time (C) and total sulfate reduction across sites (D) for the unamended treatment.

Table 2 Average \pm SD rates of denitrification (DNF), dissimilatory nitrate reduction to ammonium (DNRA), Anammox potential in nmol cm⁻³ h⁻¹ and the DNF:DNRA ratio from the Plus-NO $_3$ treatment. Different letters indicate significant differences ($\alpha = 0.05$).

Site	Week	DNF (n)	DNRA (n)	DNF	DNRA	DNF:DNRA	Anammox
Reference	8	3	4	9.84 (0.66) ^{ac}	3.96 (2.19) ^a	3.8 (2.0)	0.53 (0.21)
13-year		3	4	10.35 (2.52) ^a	3.27 (0.88) ^a	3.4 (1.4)	0.32 (0.05)
40-year		3	4	8.72 (1.99) ^{bc}	1.03 (0.55) ^b	10.7 (7.7)	0.22 (0.10)
Reference	11	3	NA	11.39 (2.89) ^{ac}	NA	NA	0.21 (0.17)
13-year		3	NA	15.03 (4.51) ^a	NA	NA	0.17 (0.05)
40-year		3	NA	8.28 (1.77) ^{bc}	NA	NA	0.11 (0.10)
Reference	12	4	4	9.81 (2.56) ^{ac}	$4.34 (0.78)^a$	2.4 (1.1)	0.14 (0.04)
13-year		4	4	13.29 (3.19) ^a	9.85 (12.62) ^a	2.8 (1.6)	0.15 (0.07)
40-year		3	3	10.02 (0.98) ^{bc}	2.11 (1.51) ^b	3.6 (0.1)	0.40 (0.26)

Table 3 Average \pm SD nitrate reduction rate (NRR) in nmol cm⁻³ h⁻¹ and the percentage (%) contribution of DNF, DNRA, and Anammox to total NRR. DNRA data were unavailable for Week 11 and were not included in calculations of % NRR.

Site	Week	NRR	% DNF of NRR	% DNRA of NRR	% Anammox of NRR	% DNF + DNRA + Ana of NRR
Reference	8	37.75 (16.01)	33.05 (1.33)	10.32 (3.37)	1.81 (0.87)	36.47 (17.15)
13-year		32.45 (5.71)	30.55 (9.45)	10.43 (3.57)	0.94 (0.23)	34.04 (17.27)
40-year		19.90 (7.13)	54.43 (17.13)	5.82 (4.34)	1.42 (0.71)	47.71 (33.86)
Reference	11	22.39 (4.32)	50.62 (14.75)	NA	0.94 (0.73)	NA
13-year		28.57 (6.82)	47.64 (6.83)	NA	0.53 (0.08)	NA
40-year		21.20 (6.55)	47.26 (17.54)	NA	0.58 (0.43)	NA
Reference	12	20.17 (9.50)	57.35 (30.31)	24.79 (10.86)	0.80 (0.21)	82.84 (35.28)
13-year		21.54 (11.04)	58.42 (35.59)	15.34 (6.54)	0.60 (0.40)	74.36 (42.53)
40-year		28.53 (9.31)	41.98 (7.11)	8.59 (6.32)	1.77 (1.12)	39.25 (27.29)

3) (Fig. 6; Table S4s; S5). Three of these ASVs (ASVs 39, 44, and 45) corresponding to the Alteromonadaceae family, and two ASVs belonging to the Gammaproteobacterial genus *Sedimenticola*, were significantly more abundant in the N addition treatment at more than one site (Fig. 5). The resulting 46 unique ASVs ranged in relative abundance only up to 4.4 % across the entire dataset.

At the reference site, in response to the NO_3^- treatment, the ASVs that increased the most dramatically were all members of the Gammaproteobacteria. In particular, ASVs in the genus *Sedimenticola* (ASVs 38, 44–45) and the family Thiotrichacaeae (ASVs 41 and 42) showed the largest increases in response to the NO_3^- addition, followed by increases in one ASV associated with the Alteromonadaceae (ASV 39). Other than Gammaproteobacteria, there was also a strong positive response to NO_3^- by an ASV from the Alphaproteobacterial genus *Rhobidium*, which is a member of the Rhizobiales order (ASV 37), and an ASV from the Betaproteobacterial family Nitrosomonadaceae (ASV 16). Three ASVs were

also inhibited by NO₃ addition from the reference site, including ASVs from two Deltaproteobacterial orders, the Desulfobacterales (ASV 35) and the Myxcoccales (ASV 34) and one genus from the Firmicutes class Clostridia (ASV 33). At the 13-year enriched site, only three ASVs were significantly enhanced under the NO₃ enrichment treatment, including the same two Sedimenticola ASVs that were enriched in reference sediments (ASV 44 and 45) and an ASV from the Thiotrichaceae (ASV 43). The addition of NO₃ did not significantly inhibit any ASVs in the 13-year enriched site. Lastly, at the 40-year enriched site, ASVs that increased as a result of NO₃ addition included ASV from the Deltaproteobacteiral family Nannocystaceae (ASV 22), the Zetaproteobacterial genus Mariprofundus (ASV 15), along with an unidentified Alphaproteobacterial ASV (ASV20), and a Gammaproteobacterial ASV from the Nitrosoccocus genus. Of the 25 ASVs in the 40-year enriched creek that responded positively to NO₃ addition, the majority were Proteobacteria, with 7 from Alphaproteobacteria, 5 from Gammaproteobacteria, 4 from

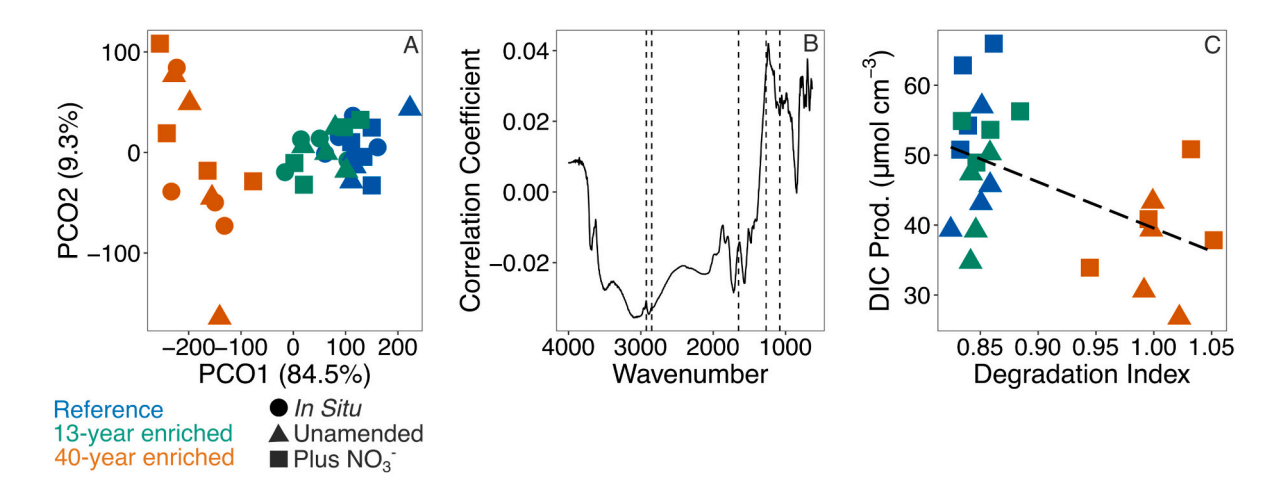


Fig. 5. (A) principal coordinates analysis of Mid-IR (infrared) spectra; (B) Pearson's correlation coefficients plotted against wavenumber representing regions most discriminating between the two axes shown in A; and (C) Total dissolved inorganic carbon (DIC) production per site as a function of the degradation index (aromatic carbon (C):carboxyl groups). Dotted lines in (B) indicate functional group assignments as follows: 840-920 and 1650 cm⁻¹ = aromatic C and lignin-type signatures, 1080 cm⁻¹ = polysaccharides, 1270 cm⁻¹ = carboxyl groups, and 2850-2924 cm⁻¹ = aliphatic C.

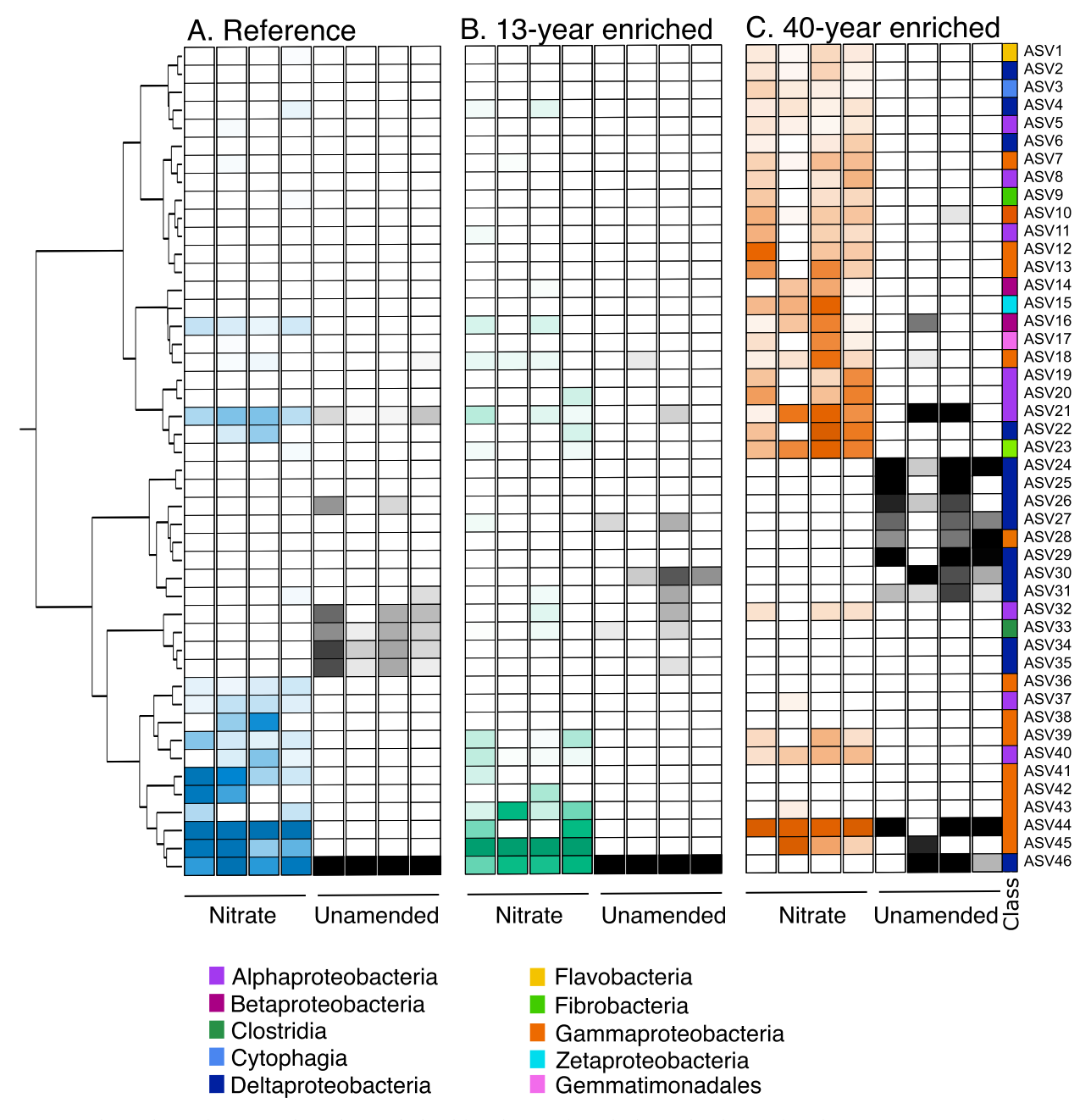


Fig. 6. Heatmaps clustered using bray-curtis dissimilarity calculated from log-transformed relative abundances of amplicon sequence variants (ASVs) found to be significantly different between unamended and plus-NO₃ treatments across reference (A), 13-year (B), and 40-year (C) enriched sites according to DESeq2. Relative abundances range from 0 to ~4.4 %, indicating significant differences occurred primarily among lower abundance taxa. Color bars indicate class-level categorization. See Supplemental Table S3 for taxonomy of individual ASVs.

Deltaproterobacteria, and 2 from Zetaproterobacteria (Fig. 6, Table S4). The Deltaproteobacteria also had 8 of the 9 ASVs that were significantly lower in abundance as a result of the NO₃ addition, including ASVs belonging to the families Desulfobacteraceae (ASV 26–27, 29), Desulfobulbaceae (ASVs 24–25, 31), Desulfarculaceae (ASV 30), and an unidentified Bacteroidetes (ASV 28).

4. Discussion

Studies of marsh loss with N enrichment have produced contradictory results with some findings that N additions enhances marsh accretion and stability, some findings suggesting it leads to marsh loss, and

others finding little effect at all (e.g. Morris et al., 2013; Deegan et al., 2012; Bowen et al., 2020; Crosby et al., 2021). All these studies have varied in the amount and form of the nitrogen additions and in the duration of the study, in addition to climate and tidal range of the salt marsh studied. Here, we used results from sites with different loading histories from within the same salt marsh to examine the legacy effect that the exposure to nutrient enrichment of varying intensities and durations has on marsh carbon degradation and microbial community structure and how that legacy might influence future ecosystem capacity to decompose organic matter under conditions of high NO_3^- exposure.

4.1. Nutrient-enriched sites contain more degraded OM and altered microbial community structure

We observed no significant differences in bulk %OM, %C, %N, and C: N ratio among the three sites exposed to different durations and concentrations of NO₃ enrichment (Table 1), however the sediments from the 40-year enriched site were characterized by significantly higher degradation index values compared to the 13-year enriched and reference sites (Fig. 1B). This degradation index, calculated as the ratio between carbon-rich aromatic compounds and oxygen-rich carboxylic compounds, is a commonly used metric to evaluate organic matter complexity, with more complex organic material having a greater accumulation of C relative to O-containing functional groups (Ding et al., 2002; Veum et al., 2013; Parikh et al., 2014; Margenot et al., 2015). One explanation for the enhanced complexity at the 40-year enriched site is that the legacy of NO₃ enrichment may have accelerated decomposition of organic matter, leaving the remaining organic material more resistant to degradation. This is supported by evidence for a NO₃-accessible pool of OM in salt marshes that is reactive under conditions of high NO₃ but not in the presence of anoxic seawater alone (Bulseco et al., 2019). Sites experiencing chronic NO₃ enrichment may therefore demonstrate higher rates of decomposition during initial OM deposition, thereby resulting in the accumulation of less biologically available OM over time.

Differences in OM quality among our sites may be due to differences in their respective microbial communities or vice versa. We observed significant site-specific differences in the community structure of the active microbes (Fig. 2). All three sites were dominated by two families of active bacterial taxa — the Campylobacteraceae and the Oceanospirillaceae. However, the Campylobacteraceae family decreased in relative abundance with chronic NO3 exposure while the Oceanospirillaceae increased slightly. In this study, all ASVs associated with Campylobacteraceae belonged to the genus Arcobacter, previously identified to contain N-fixing taxa associated with the roots of the salt marsh grass Spartina alterniflora (Pati et al., 2010). N2-fixation rates in salt marshes can decrease with increasing N supply (Howarth et al., 1988), consistent with this difference in Arcobacter relative abundance we observed. The reference and 13-year enriched site also had a higher proportion of Desulfobacteraceae, Psychromonadaceae, and Vibrionaceae than the 40-year enriched site. Desulfobacteraceae contain a wide array of taxa known to reduce SO₄²⁻ (Klepac-Ceraj et al., 2004; Bahr et al., 2005), thus their low abundance in the 40-year enriched site may indicate a shift toward greater use of NO_3^- , rather than SO_4^{2-} , as an electron acceptor at the chronically NO₃ enriched site. Both Psychomonadaceae and Vibrionaceae can proliferate in areas with large amounts of organic carbon (Thingstad et al., 2022), a mechanism that might explain their lower relative abundance in the 40-year enriched site where the residual organic matter is more degraded than the other sites (Fig. 2). By contrast, the 40-year enriched site had higher relative proportions of Pseudomonadaceae and Rhodocyclaceae compared to the reference and 13-year enriched site (Fig. 2). Both families are associated with degradation of complex aromatic carbon structures including petroleum-derived contaminants (Sun et al., 2022), polycyclic aromatic hydrocarbons (Corteselli et al., 2017), and toluene (Tancsics et al., 2018). This degradation of complex carbon is frequently coupled with nitrate reduction (Mikes et al., 2021; Shen et al., 2022; Sun et al., 2022). Thus, these taxa may be able to use high NO_3^- concentrations to facilitate further degradation of the residual organic material at the 40-year enriched site.

Differences in the microbial community could also be due to salinity differences among our sites (Table 1), however, the most significant salinity-induced changes to typical estuarine microbial communities typically occur at low salinities (below \sim 5 ppt). This is where dramatic shifts in ammonium adsorption can occur (Weston et al., 2010) and where anaerobic metabolisms can shift from methanogenesis to SO_4^- reduction (Chambers et al., 2011; Poffenbarger et al., 2011; Vizza et al.,

2017). Salinity was lower and more variable at the 40-year enriched site, compared to the reference and 13-year enriched sites. However, the same taxa associated with SO₄ reduction decreased in both the 13-year, which had the highest salinity, and the 40-year enriched site with the lowest salinity, suggesting that salinity was less important than nutrient enrichment in driving this pattern (Fig. 2). Further, the reference site, where ASVs associated with SO₄ reduction were highest, had intermediate salinity (Table 1), suggesting salinity differences likely play only a minor role in structuring the microbial communities in these three sites. Lastly, differences in the degree of degradation of the organic matter at the 40-year enriched site could also be a result of differences due to other material released in the water from the upstream wastewater treatment plant and variability of salinity at the 40-year enriched site. Graves et al. (2016) found evidence in the metagenomic profiles that genes related to osmotic stress and phage resistance were influenced by exposure to sewage effluent. However, taken together, the microbial communities at these sites reflect expectations, with a higher proportion of SO₄ reducing and N-fixing taxa in the reference site and communities specialized in nitrate reduction and complex aromatic carbon degradation in the 40-year enriched site.

4.2. The nitrate-accessible pool of OM is smaller at nutrient enriched sites

We hypothesized that if chronically enriched sites contained taxa more adapted to high N conditions and more chemically complex OM, as suggested by our taxonomic analysis (Fig. 2), then these communities would not respond as strongly to further NO₃ addition when compared to the reference site. Although the addition of NO₃ resulted in significantly greater DIC production compared to the unamended treatment at all sites (Fig. 3), the effect size was lowest at the 40-year enriched site, supporting our hypothesis. Lower microbial respiration rates suggest that the NO3-accessible pool of OM is smaller at the 40-year enriched site, presumably because a larger fraction of OM was already oxidized. In the reference site, where more of the NO₃-accessible OM pool was still intact, there was greater DIC production from these sediments when NO₃ was experimentally provided (Fig. 3), which resulted in the greatest cumulative loss of total C (Fig. 3E), and a significant decrease in %C between untreated and plus-NO₃ sediments at the end of the experiment (Table 1). Despite increases in respiration across all our sites, the FT-IR spectral data (Fig. 5) support the idea that the legacy of nutrient enrichment was more important to the structure of the organic matter pool than the short-term NO_{3}^{-} addition in our flow through reactor experiment, as indicated by the lack of differentiation between the unamended and plus- NO₃ treatments (Fig. 5).

Under anaerobic conditions when there is ample NO_3^- two competing dissimilatory NO_3^- reduction pathways, denitrification (DNF) and dissimilatory nitrate reduction to ammonium (DNRA), can be used by microbes to facilitate respiration, and the composition of the organic matter can play an important role in determining the balance between DNF and DNRA. Theoretical models predict that under conditions of low organic matter to NO_3^- ratios, DNF will predominate because it provides more free energy per mole of C oxidized than DNRA (Giblin et al., 2013; Algar and Vallino, 2014). Additionally, Koop-Jakobsen and Giblin (2010) showed that in creek sediments from the same 13-year enriched site used here, nutrient enrichment increased DNF by 16 fold when compared to the reference site, whereas DNRA only increased 10-fold, indicating a preference for DNF under high NO3 conditions.

In our experiment, we held NO_3^- concentrations constant across all three sites to assess whether the increased degradation of organic matter as a result of chronic NO_3^- exposure would shift the relative proportion of DNF and DNRA. We found that DNRA was lower at the 40-year enriched site than both the reference and 13-year enriched sites, resulting in DNF:DNRA ratios that were highest at the 40-year marsh (Table 2) where the degradation index was the highest (Fig. 1). These results indicate that under constant NO_3^- supply and a range of organic matter qualities, DNF is strongly preferred over DNRA in systems with

low quality organic matter. This distinction is important because DNF reduces NO_3^- to N_2 gas where it escapes from the environment whereas DNRA reduces NO_3^- to NH_4^+ , retaining it in the system where it can continue to promote primary production (Giblin et al., 2013).

Although both DNF and DNRA can be used to promote decomposition of organic matter under high NO₃ conditions, they can also both be used for autotrophic growth when coupled with oxidation of reduced compounds (Burgin and Hamilton, 2007), though measuring DNF and DNRA alone cannot differentiate between autotrophic and heterotrophic processes. However, stoichiometric ratios can provide insight. We calculated the mass balance between DIC production and $NO_3^- + SO_4^{2-}$ reduction in the plus-NO₃ treatment and the ratios were considerably lower than the predicted stoichiometry. This indicates that either 1) NO₃ is being consumed by assimilation or 2) chemoautotrophic microbes are fixing DIC, potentially using NO₃ as an electron acceptor, or both. Although a small amount of NO₃ assimilation could be occurring, the energetic requirements for microbes to assimilate NH₄ is lower than for NO₃ assimilation when there is sufficient NH₄ present. Our reactor experiments produced small amounts of NH₄ across all sites in both the plus NO₃ and unamended treatments (Fig. S3), suggesting that the N demand for microbial assimilation was likely already being met, and reducing the likelihood that microbes would assimilate NO₃. Further, anaerobic microbes are seldom nutrient-limited because their growthper-unit substrate-intake is much lower than for aerobic microbes (Canfield et al., 2005). Chemoautotrophic processes, on the other hand, could include NO₃ reduction coupled to the oxidation of reduced S and/ or iron (Burgin and Hamilton, 2007; Giblin et al., 2013) and both substrates are abundant in these marsh sediments. Both processes fix DIC and would result in lower DIC production relative to NO₃ consumption than expected by heterotrophic, dissimilatory nitrate reduction stoichiometry. Metagenomic data from previous NO3 enrichment experiments support this hypothesis, demonstrating a significant increase in genes associated with CO2 fixation in a different NO3 addition experiment (Bulseco et al., 2020). Reconstruction of microbial genomes from metagenomic data in that same study indicated that the full biochemical pathways for carbon fixation through both the Wood Ljungdahl and Calvin Benson Bassham pathways (Vineis et al., 2023) were present, providing additional support for the role of chemoautotrophic DNF and DNRA in this system.

4.3. NO_3^- addition shifts microbial community structure and activity regardless of prior exposure

Initial sediments from the 13-year and 40-year enriched sites contained taxa that may have been selected for because of the legacy of N enrichment (Fig. 2), so we hypothesized that further NO₃ addition would not alter the active microbial community structure compared to the unamended treatment. Whereas the microbial community at the reference site, having no chronic prior exposure to high NO₃ concentrations, would display a greater shift in microbial community structure in response to experimental NO₃ addition. Our results indicate that the site-specific differences in the active community persisted through our NO3 addition experiment and there was a significant treatment effect across all sites. But the dispersion in the active microbial community at the 40-enriched site was considerably higher than in the other two sites, making site specific treatment effects difficult to discern (Fig. S2). However, significant differences in the relative abundances of taxa between the NO₃ addition and unamended cores within each site suggest that many taxa showed significant strong positive or negative responses to the experimental NO₃ addition (Fig. 6).

Three ASVs were significantly enriched in more than one site, including one unidentified member of the Alteromonadales and two ASVs belonging to the typically chemoautotrophic Gammaproteo-bacterial genus Sedimenticola, which were also previously identified in NO_3^- enriched bioreactors (Vineis et al., 2023). Genomes of Sedimenticola derived from shotgun metagenomic data indicate the capacity for

complete denitrification coupled with sulfur oxidation, along with genes for both autotrophic and heterotrophic metabolisms (Vineis et al., 2023), suggesting they have versatile metabolisms that allow them to thrive under high NO_3^- conditions. *Sedimenticola* were previously isolated from salt marsh (Flood et al., 2015) and estuarine (Narasingarao and Haggblom, 2006) sediments, further supporting their ubiquity and potential importance in coastal sediments.

Most taxa that were significantly different between the NO₃ addition and unamended reactors were found in sediments collected from the 40year enriched site, in contrast to our expectation that these sediments would diverge the least as a result of our treatment. Active taxa that increased their relative abundance in the NO_3^- addition from the 40-year enriched habitats included taxa with members involved in biogeochemical cycling of nitrogen. Surprisingly, several ASVs that were relatively more abundant in the NO₃ addition treatment from the chronically enriched site belonged to clades with the capacity for ammonia oxidation, including ASVs from the Chromatiales genus Nitrosococcus and from the Betaprotoeobacterial family Nitrosomonadaceae. Ammonia oxidation rates can be high in salt marshes, particularly in the tall ecotype of Spartina alterniflora (Dollhopf et al., 2005) where these samples were collected. Compared to the other sites, in the 40-year enriched sites we observed lower rates of DNRA and lower incremental increases in DIC production, both of which would suggest lower supplies of NH₄⁺ that could be used to fuel ammonia oxidation. Indeed, NH₄ production rates were lowest in the 40-year enriched plus-NO₃ treatment (Fig. S3), though measurable quantities of NH₄ persisted throughout the experiment in all treatments. The decomposition experiment was carried out under anaerobic conditions, which should also inhibit ammonium oxidation, making it perplexing that multiple ASVs across two distinct clades of ammonia oxidizers were enriched in the NO₃ addition treatment, although we did detect low rates of anammox throughout the experiment (Table 2). Additionally, the presence of the iron oxidizing Zetaproteobacteria Mariprofundus, also thought to be an obligate microaerophile (Singer et al., 2011), further suggests that there must be a supply of O2 available in these reactors. Oxygen concentrations in our experiment were maintained below the limit of detection of the oxygen sensor used to monitor concentrations, raising the possibility of some non-photosynthetic source of O2 supply, as was recently demonstrated by the ammonia oxidizing archaea Nitrosopumulis maritimus (Kraft et al., 2022) or through nitric oxide dismutation (Ettwig et al., 2012)..

In sediments from the reference site, we also observed several taxa that responded positively to the NO₃ addition. However, there was little overlap between the ASVs that were significantly enhanced due to NO₃ addition in the reference sediments compared to the 40-year enriched sediments, except Sedimenticola, which was enriched at both sites. The taxa enriched from the reference site largely belonged to the orders Thiotrichales and Rhizobiales. The Thiotrichales contain the genera Thioploca and Beggiatoa both of which can undergo anaerobic sulfide oxidation using vacuole-stored NO₃ as an electron acceptor (Kamp et al., 2006; Callbeck et al., 2021) and are known to dominate salt marsh sulfur oxidation (Thomas et al., 2014). The Rhizobiales are a polyphyletic group of Alphaproteobacteria often found in salt marsh rhizospheres (Dini-Andreote et al., 2016; Kearns et al., 2016; Lynum et al., 2020). By contrast, the active taxa that were most abundant in the unamended treatment, where no NO3 was added, were largely all members of the Desulfobacterales, which are widespread SO₄²⁻ reducers that are also commonly found in salt marsh sediments (Bahr et al., 2005; Bulseco et al., 2019; Bulseco et al., 2020).

5. Conclusions

We show that reference and 13-year enriched marshes exhibited similar OM composition and microbial community structure, and that the 40-year enriched marsh was characterized by more highly degraded organic matter and a unique microbial community compared to the other two sites. After exposing sediments to additional NO_3^- in a controlled reactor experiment, the reference site exhibited the greatest difference in rates of DIC production compared to the unamended control. In contrast, sediments from the 40-year enriched site demonstrated a lower response to NO_3^- , despite significant changes to both microbial community structure and activity. These results suggest that the fraction of OM buried in sediments under long term NO_3^- enrichment may be more stable when compared to less N-enriched systems. Our work highlights the need to consider the effects of chronic nutrient enrichment when determining C storage potential in salt marsh systems.

Funding

This work was funded by an NSF CAREER Award to JLB (DEB1350491), a NSF OCE award to AEG for the Plum Island Ecosystems LTER (OCE1637630), a Woods Hole Oceanographic Sea Grant award to AEG (Project No. NA140AR4170074 Project R/M-65s), an NSF DDIG award to ANB and JLB (DEB1701748), an NSF PRBF award to AB (NSF 1907285), and an additional NSF award to JLB and AEG (DEB 2203322). Additional support was provided by a Ford Foundation predoctoral fellowship award to ANB. The views expressed here are those of the authors and do not necessarily reflect the views of NOAA or any of is subagencies.

CRediT authorship contribution statement

Ashley N. Bulseco: Conceptualization, Data curation, Formal analysis, Investigation, Methodology, Visualization, Writing – original draft, Writing – review & editing. Anna E. Murphy: Formal analysis, Investigation, Methodology, Writing – review & editing. Anne E. Giblin: Conceptualization, Funding acquisition, Project administration, Supervision, Validation, Writing – review & editing. Jane Tucker: Investigation, Methodology, Validation, Writing – review & editing. Jonathan Sanderman: Formal analysis, Investigation, Resources, Software, Writing – review & editing. Jennifer L. Bowen: Conceptualization, Funding acquisition, Project administration, Resources, Supervision, Validation, Writing – original draft, Writing – review & editing.

Declaration of competing interest

The authors declare that they have no known competing financial interests or personal relationships that could have appeared to influence the work reported in this paper.

Data availability

Sequence data are available on the NCBI Sequence Read Archive under BioProject ID PRJNA1014411 and the remaining data are available on the Plum Island Ecosystems LTER website (http://pie-lter.ecosystems.mbl.edu/data-research-area).

Acknowledgements

We would like to thank Joseph Vallino at Marine Biological Laboratory and Gary Banta at Roskilde University for their thoughtful contribution to our experiment as well as Tom Goodkind at the University of Massachusetts Boston for flow through reactor design and construction. We also thank researchers of the TIDE project (NSF OCE0924287, OCE0923689, DEB0213767, DEB1354494, and OCE 1353140) for maintenance of the long-term nutrient enrichment experiment and researchers at the Plum Island Ecosystems LTER (NSF OCE 0423565, 1058747, 1637630) for logistical support. Thanks to Sam Kelsey at the Marine Biological Laboratory and Alan Stebbins at University of Massachusetts Boston Environmental Analytical Facility for assistance in the laboratory. Lastly, we thank Chris Reddy for the use of the anaerobic chamber at the Woods Hole Oceanographic Institution

and Amanda Spivak for the resource support.

Appendix A. Supplementary data

Supplementary data to this article can be found online at https://doi.org/10.1016/j.scitotenv.2023.169681.

References

- Algar, C.K., Vallino, J.J., 2014. Predicting microbial nitrate reduction pathways in coastal sediments. Aquat. Microb. Ecol. 71, 223–238. https://doi.org/10.3354/ ame01678
- Angell, J.H., Peng, X., Ji, Q., Craick, I., Jayakumar, A., Kearns, P.J., Ward, B.B., Bowen, J. L., 2018. Community composition of nitrous oxide-related genes in salt marsh sediments exposed to nitrogen enrichment. Front. Microbiol. 9, 170. https://doi.org/10.3389/fmicb.2018.00170.
- Bahr, M., Crump, B.C., Klepac-Ceraj, V., Teske, A., Sogin, M.L., Hobbie, J.E., 2005. Molecular characterization of sulfate-reducing bacteria in a New England salt marsh. Environ. Microbiol. 7, 1175–1185. https://doi.org/10.1111/j.1462-2920.2005.00796.x.
- Bates, S.T., Berg-Lyons, D., Caporaso, J.G., Walters, W.A., Knight, R., Fierer, N., 2011. Examining the global distribution of dominant archaeal populations in soil. ISME J. 5, 908–917. https://doi.org/10.1038/ismej.2010.171.
- Bowen, J.L., Crump, B.C., Deegan, L.A., Hobbie, J.E., 2009. Salt marsh sediment bacteria: their distribution and response to external nutrient inputs. ISME J. 3, 924–934. https://doi.org/10.1038/ismej.2009.44.
- Bowen, J.L., Byrnes, J.E., Weisman, D., Colaneri, C., 2013. Functional gene pyrosequencing and network analysis: an approach to examine the response of denitrifying bacteria to increased nitrogen supply in salt marsh sediments. Front. Microbiol. 4, 342. https://doi.org/10.3389/fmicb.2013.00342.
- Bowen, J.L., Giblin, A.E., Murphy, A.E., Bulseco, A.N., Deegan, L.A., Johnson, D.S., Nelson, J.A., Mozdzer, T.J., Sullivan, H.L., 2020. Not all nitrogen is created equal: differential effects of nitrate and ammonium enrichment in coastal wetlands. BioScience 70, 1108–1119. https://doi.org/10.1093/biosci/biaal40.
- Bricker, S.B., Longstaff, B., Dennison, W., Jones, A., Boicourt, K., Wicks, C., Woerner, J., 2008. Effects of nutrient enrichment in the nation's estuaries: a decade of change. Harmful Algae 8, 21–32. https://doi.org/10.1016/j.hal.2008.08.028.
- Bulseco, A.N., Giblin, A.E., Tucker, J., Murphy, A.E., Sanderman, J., Hiller-Bittrolff, K., Bowen, J.L., 2019. Nitrate addition stimulates microbial decomposition of organic matter in salt marsh sediments. Glob. Chang. Biol. 25, 3224–3241. https://doi.org/ 10.1111/cph.14726
- Bulseco, A.N., Vineis, J.H., Murphy, A.E., Spivak, A.C., Giblin, A.E., Tucker, J., Bowen, J. L., 2020. Metagenomics coupled with biogeochemical rates measurements provide evidence that nitrate addition stimulates respiration in salt marsh sediments. Limnol. Oceanogr. 65, S321–S339. https://doi.org/10.1002/lno.11326.
- Burdige, D., 2007. Preservation of organic matter in marine sediments: controls, mechanisms, and an imbalance in sediment organic carbon budgets? Chem. Rev. 107, 467–485. https://doi.org/10.1021/cr050347q.
- Burgin, A. J., and S. K. Hamilton. 2007. Have we overemphasized the role of denitrification in aquatic ecosystems? A review of nitrate removal pathways. Front. Ecol. Environ. 5:89–96. doi:https://doi.org/10.1890/1540-9295(2007)5[89, HWOTRO]2.0.CO;2.
- Callahan, B.J., McMurdie, P.J., Rosen, M.J., Han, A.W., Johnson, A.J., Holmes, S.P., 2016. DADA2: high-resolution sample inference from Illumina amplicon data. Nat. Methods 13, 581–583. https://doi.org/10.1038/nmeth.3869.
- Callbeck, C.M., Canfield, D.E., Kuypers, M.M.M., Yilmaz, P., Lavik, G., Thamdrup, B., Schubert, C.J., Bristow, L.A., 2021. Sulfur cycling in oceanic oxygen minimum zones. Limnol. Oceanogr. 66, 2360–2392. https://doi.org/10.1002/lno.11759.
- Canfield, D.E., Thamdrup, B., Kristensen, E., 2005. Aquatic Geomicrobiology. Elsevier Academic Press, Boston, MA.
- Caporaso, J.G., Kuczynski, J., Stombaugh, J., Bittinger, K., Bushman, F.D., Costello, E.K., Fierer, N., Gonzalez Pena, A., Goodrich, J.K., Gordon, J.I., Huttley, G.A., Kelley, S.T., Knights, D., Koenig, J.E., Ley, R.E., Lozupone, C.A., McDonald, D., Muegge, B., Pirrung, M., Reeder, J., Sevinsky, J.R., Turnbaugh, P.J., Walters, W.A., Widmann, J., Yatsunenko, T., Zaneveld, J., Knight, R., 2010. QIIME allows analysis of high-throughput community sequencing data. Nat. Methods 7, 335–336. https://doi.org/10.1038/mmeth.f.303.
- Caporaso, J.G., Lauber, C.L., Walters, W.A., Berg-Lyons, D., Lozupone, C.A., Turnbaugh, P.J., Fierer, N., Knight, R., 2011. Global patterns of 16S rRNA diversity at a depth of millions of sequences per sample. Proc. Natl. Acad. Sci. U. S. A. 108, 4516–4522. https://doi.org/10.1073/pnas.1000080107.
- Caporaso, J.G., Lauber, C.L., Walters, W.A., Berg-Lyons, D., Huntley, J., Fierer, N., Owens, S.M., Betley, J., Fraser, L., Bauer, M., Gormley, N., Gilbert, J.A., Smith, G., Knight, R., 2012. Ultra-high-throughput microbial community analysis on the Illumina HiSeq and MiSeq platforms. ISME J. 6, 1621–1624. https://doi.org/ 10.1038/ismej.2012.8.
- Chambers, L.G., Reddy, K.R., Osborne, T.Z., 2011. Short-term response of carbon cycling to salinity pulses in a freshwater wetland. Soil Sci. Soc. Am. J. 75, 2000–2007. https://doi.org/10.2136/sssaj2011.0026.
- Chmura, G.L., Anisfeld, S.C., Cahoon, D.R., Lynch, J.C., 2003. Global carbon sequestration in tidal, saline wetland soils. Global Biogeochem. Cycles 17, 22. https://doi.org/10.1029/2002GB001917.

- Conant, R. T., M. G. Ryan, G. I. Ågren, H. E. Birge, E. A. Davidson, P. E. Eliasson, S. E. Evans, S. D. Frey, C. P. Giardina, F. M. Hopkins, R. Hyvönen, M. U. F.
- Corteselli, E.M., Aitken, M.D., Singleton, D.R., 2017. Rugosibacter aromaticivoransgen. nov., sp. nov., a bacterium within the family Rhodocyclaceae, isolated from contaminated soil, capable of degrading aromatic compounds. Int. J. Syst. Evol. Microbiol. 67, 311–318. https://doi.org/10.1099/ijsem.0.001622.
- Cox, R.D., 1980. Determination of nitrate and nitrite at the parts per billion level by chemiluminescence. Anal. Chem. 52, 332–335.
- Crosby, S.C., Spiller, N.C., Healy, D.S., Brideau, L., Stewart, L.M., Vaudrey, J.M.P., Tietz, K.E., Fraboni, P.J., 2021. Assessing the resiliency of salt marshes under increasing nitrogen loading. Estuar. Coasts 44, 1658–1670. https://doi.org/10.1007/s12237-021-00899-1.
- Deegan, L.A., Bowen, J.L., Drake, D., Fleeger, J.W., Friedrichs, C.T., Galván, K.A., Hobbie, J.E., Hopkinson, C.S., Johnson, D.S., Johnson, J.M., LeMay, L.E., Miller, E., Peterson, B.J., Picard, C., Sheldon, S., Sutherland, M., Vallino, J.J., Warren, R.S., 2007. Susceptibility of salt marshes to nutrient enrichment and predation removal. Ecol. Appl. 17, 42–63. https://doi.org/10.1890/06-0452.1.
- Deegan, L.A., Johnson, D.S., Warren, R.S., Peterson, B.J., Fleeger, J.W., Fagherazzi, S., Wollheim, W.M., 2012. Coastal eutrophication as a driver of salt marsh loss. Nature 490, 388–392. https://doi.org/10.1038/nature11533.
- Ding, G., Novak, J.M., Amarasiriwardena, D., Hunt, P.G., Xing, B., 2002. Soil organic matter characteristics as affected by tillage management. Soil Sci. Soc. Am. J. 66, 421–429. https://doi.org/10.2136/sssaj2002.4210.
- Dini-Andreote, F., Brossi, M.J., van Elsas, J.D., Salles, J.F., 2016. Reconstructing the genetic potential of the microbially-mediated nitrogen cycle in a salt marsh ecosystem. Front. Microbiol. 7, 902. https://doi.org/10.3389/fmicb.2016.00902.
- Dollhopf, S.L., Hyun, J.H., Smith, A.C., Adams, H.J., O'Brien, S., Kostka, J.E., 2005. Quantification of ammonia-oxidizing bacteria and factors controlling nitrification in salt marsh sediments. Appl. Environ. Microbiol. 71, 240–246. https://doi.org/ 10.1128/AEM.71.1.240-246.2005.
- Eren, A.M., Esen, O.C., Quince, C., Vineis, J.H., Morrison, H.G., Sogin, M.L., Delmont, T. O., 2015. Anvi'o: an advanced analysis and visualization platform for 'omics data. PeerJ 3, e1319. https://doi.org/10.7717/peerj.1319.
- Ettwig, K.F., Speth, D.R., Reimann, J., Wu, M.L., Jetten, M.S., Keltjens, J.T., 2012. Bacterial oxygen production in the dark. Front. Microbiol. 3, 273. https://doi.org/ 10.3389/fmicb.2012.00273.
- Eyre, B. D., S. Rysgaard, T. Dalsgaard, and P. B. Christensen. 2002. Comparison of isotope pairing and N2:Ar methods for measuring sediment denitrification—assumptions, modifications, and implications. Estuaries 25: 1077–1087. doi:https://doi.org/10.1007/BF02692205.
- Flood, B.E., Jones, D.S., Bailey, J.V., 2015. Sedimenticola thiotaurini sp. nov., a sulfur-oxidizing bacterium isolated from salt marsh sediments, and emended descriptions of the genus Sedimenticola and Sedimenticola selenatireducens. Int. J. Syst. Evol. Microbiol. 65, 2522–2530. https://doi.org/10.1099/ijs.0.000295.
- Galloway, J.N., Townsend, A.R., Erisman, J.W., Bekunda, M., Cai, Z., Freney, J.R., Martinelli, L.A., Seitzinger, S.P., Sutton, M.A., 2008. Transformation of the nitrogen cycle: recent trends, questions, and potential solutions. Science 320, 889–892. https://doi.org/10.1126/science.1136674.
- Galloway, J.N., Leach, A.M., Erisman, J.W., Bleeker, A., 2017. Nitrogen: the historical progression from ignorance to knowledge, with a view to future solutions. Soil Res. 55. 417–424. https://doi.org/10.1071/SR16334.
- Giblin, A., Tobias, C., Song, B., Weston, N., Banta, G., Rivera-Monroy, V., 2013. The importance of dissimilatory nitrate reduction to ammonium (DNRA) in the nitrogen cycle of coastal ecosystems. Oceanography 26, 124–131. https://doi.org/10.5670/ oceanog.2013.54.
- Gilboa-Garber, N., 1971. Direct spectrophotometric determination of inorganic sulfide in biological materials and in other complex mixtures. Anal. Biochem. 43, 129–133. https://doi.org/10.1016/0003-2697(71)90116-3
- Graves, C.J., Makrides, E.J., Schmidt, V.T., Giblin, A.E., Cardon, Z.G., Rand, D.M., 2016. Functional responses of salt marsh microbial communities to long-term nutrient enrichment. Appl. Environ. Microbiol. 82, 2862–2871. https://doi.org/10.1128/ AFM.03990-15.
- Hardison, A.K., Algar, C.K., Giblin, A.E., Rich, J.J., 2015. Influence of organic carbon and nitrate loading on partitioning between dissimilatory nitrate reduction to ammonium (DNRA) and N2 production. Geochim. Cosmochim. Acta 164, 146–160. https://doi.org/10.1016/j.gca.2015.04.049.
- Howarth, R.W., Marino, R., Cole, J.J., 1988. Nitrogen fixation in freshwater, estuarine, and marine ecosystems. 2. Biogeochemical controls. Limnol. Oceanogr. 33, 688–701. https://doi.org/10.4319/lo.1988.33.4part2.0688.
- Kamp, A., Stief, P., Schulz-Vogt, H.N., 2006. Anaerobic sulfide oxidation with nitrate by a freshwater Beggiatoa enrichment culture. Appl. Environ. Microbiol. 72, 4755–4760. https://doi.org/10.1128/AEM.00163-06.
- Kana, T.M., Darkangelo, C., Hunt, M.D., Oldham, J.B., Bennett, G.E., C. J. C., 1994.
 Membrane inlet mass spectrometer for rapid high-precision determination of N2, O2, and Ar in environmental water samples. Anal. Chem. 66, 4166–4170. https://doi.org/10.1021/ar000953009
- Kearns, P.J., Angell, J.H., Howard, E.M., Deegan, L.A., Stanley, R.H., Bowen, J.L., 2016. Nutrient enrichment induces dormancy and decreases diversity of active bacteria in salt marsh sediments. Nat. Commun. 7, 12881. https://doi.org/10.1038/ ncomms12881.
- Kearns, P.J., Bulseco-McKim, A.N., Hoyt, H., Angell, J.H., Bowen, J.L., 2019. Nutrient enrichment alters salt marsh fungal communities and promotes putative fungal denitrifiers. Microb. Ecol. 77, 358–369. https://doi.org/10.1007/s00248-018-1223-

- Kirschbaum, M.U.F., 1995. The temperature dependence of soil organic matter decomposition, and the effect of global warming on soil organic carbon storage. Soil Biol. Biochem. 27, 753–760. https://doi.org/10.1016/0038-0717(94)00242-8.
- Kirschbaum, J.M., Lavallee, J., Leifeld, W.J., Parton, J. Megan, Steinweg, M.D., Wallenstein, J.Å., Wetterstedt, Martin, Bradford, M.A., 2011. Temperature and soil organic matter decomposition rates - synthesis of current knowledge and a way forward. Glob. Chang. Biol. 17, 3392–3404. https://doi.org/10.1111/j.1365-2486.2011.02496.x
- Kirwan, M.L., Langley, J.A., Guntenspergen, G.R., Megonigal, J.P., 2013. The impact of sea-level rise on organic matter decay rates in Chesapeake Bay brackish tidal marshes. Biogeosciences 10, 1869–1876. https://doi.org/10.5194/bg-10-1869-2013
- Klepac-Ceraj, V., Bahr, M., Crump, B.C., Teske, A.P., Hobbie, J.E., Polz, M.F., 2004. High overall diversity and dominance of microdiverse relationships in salt marsh sulphate-reducing bacteria. Environ. Microbiol. 6, 686–698. https://doi.org/ 10.1111/j.1462-2920.2004.00600.x.
- Koop-Jakobsen, K., Giblin, A.E., 2010. The effect of increased nitrate loading on nitrate reduction via denitirification and DNRA in salt marsh. Limnol. Oceanogr. 55, 789–802. https://doi.org/10.4319/lo.2010.55.2.0789.
- Kraft, B., Jehmlich, N., Larsen, M., Bristow, L.A., Konneke, M., Thamdrup, B., Canfield, D.E., 2022. Oxygen and nitrogen production by an ammonia-oxidizing archaeon. Science 375, 97–100. https://doi.org/10.1126/science.abe6733.
- Langley, A. J., T. J. Mozdzer, K. A. Shepard, S. B. Hagerty, and J. Patrick Megonigal. 2013. Tidal marsh plant responses to elevated CO2, nitrogen fertilization, and sea level rise. Glob. Chang. Biol. 19:1495–1503. doi:https://doi.org/10.1111/ gcb.12147.
- Ledford, T.C., Mortazavi, B., Tatariw, C., Mason, O.U., 2020. Elevated nutrient inputs to marshes differentially impact carbon and nitrogen cycling in two northern Gulf of Mexico saltmarsh plants. Biogeochemistry 149, 1–16. https://doi.org/10.1007/ s10533-020-00656-9.
- Lehmann, J., Kleber, M., 2015. The contentious nature of soil organic matter. Nature 528, 60–68. https://doi.org/10.1038/nature16069.
- Lloret, J., Valiela, I., 2016. Unprecedented decrease in deposition of nitrogen oxides over North America: the relative effects of emission controls and prevailing air-mass trajectories. Biogeochemistry 129, 165–180. https://doi.org/10.1007/s10533-016-0225-5
- Love, M.I., Huber, W., Anders, S., 2014. Moderated estimation of fold change and dispersion for RNA-seq data with DESeq2. Genome Biol. 15, 550. https://doi.org/ 10.1186/s13059-014-0550-8.
- Lunstrum, A., Aoki, L.R., 2016. Oxygen interference with membrane inlet mass spectrometry may overestimate denitrification rates calculated with the isotope pairing technique. Limnol. Oceanogr. Methods 14, 425–431. https://doi.org/ 10.1002/jom3.10101.
- Lynum, C.A., Bulseco, A.N., Dunphy, C.M., Osborne, S.M., Vineis, J.H., Bowen, J.L., 2020. Microbial community response to a passive salt marsh restoration. Estuar. Coasts 43, 1439–1455. https://doi.org/10.1007/s12237-020-00719-y.
- Margenot, A.J., Calderón, F.J., Bowles, T.M., Parikh, S.J., Jackson, L.E., 2015. Soil organic matter functional group composition in relation to organic carbon, nitrogen, and phosphorus fractions in organically managed tomato fields. Soil Sci. Soc. Am. J. 79, 772–782. https://doi.org/10.2136/sssaj2015.02.0070.
- Martin, R.M., Wigand, C., Elmstrom, E., Lloret, J., Valiela, I., 2018. Long-term nutrient addition increases respiration and nitrous oxide emissions in a New England salt marsh. Ecol. Evol. 8, 4958–4966. https://doi.org/10.1002/ece3.3955.
- McMurdie, P.J., Holmes, S., 2013. Phyloseq: an R package for reproducible interactive analysis and graphics of microbiome census data. PloS One 8, e61217. https://doi. org/10.1371/journal.pone.0061217.
- Mettel, C., Kim, Y., Shrestha, P.M., Liesack, W., 2010. Extraction of mRNA from soil. Appl. Environ. Microbiol. 76, 5995–6000. https://doi.org/10.1128/AEM.03047-09.
- Mikes, M.C., Martin, T.K., Moe, W.M., 2021. Azospira inquinata sp. nov., a nitrate-reducing bacterium of the family Rhodocyclaceae isolated from contaminated groundwater. Int. J. Syst. Evol. Microbiol. 71, 005172 https://doi.org/10.1099/ijcap.0.005172
- Morris, J.T., 1991. Effects of nitrogen loading on wetland ecosystems with particular reference to atmospheric deposition. Annu. Rev. Ecol. Syst. 22, 257–279. https://doi.org/10.1146/annurev.es.22.110191.001353.
- Morris, J. T., G. P. Shaffer, and J. A. Nyman. 2013. Brinson review: perspectives on the influence of nutrients on the sustainability of coastal wetlands. Wetlands 33: 975–988. doi:https://doi.org/10.1007/s13157-013-0480-3.
- Mueller, P., Schile-Beers, L.M., Mozdzer, T.J., Chmura, G.L., Dinter, T., Kuzyakov, Y., de Groot, A.V., Esselink, P., Smit, C., D'Alpaos, A., Ibáñez, C., Lazarus, M., Neumeier, U., Johnson, B.J., Baldwin, A.H., Yarwood, S.A., Montemayor, D.I., Yang, Z., Wu, J., Jensen, K., Nolte, S., 2018. Global-change effects on early-stage decomposition processes in tidal wetlands implications from a global survey using standardized litter. Biogeosciences 15, 3189–3202. https://doi.org/10.5194/bg-15-3189-2018.
- Narasingarao, P., Haggblom, M.M., 2006. Sedimenticola selenatireducens, gen. nov., sp. nov., an anaerobic selenate-respiring bacterium isolated from estuarine sediment. Syst. Appl. Microbiol. 29, 382–388. https://doi.org/10.1016/j.syapm.2005.12.011.
- Nielsen, L.P., 1992. Denitrification in sediment determined from nitrogen isotope pairing. FEMS Microbiol. Ecol. 86, 357–362. https://doi.org/10.1111/j.1574-6069.1009.bbs/29.pr.
- Pallud, C., Van Cappellen, P., 2006. Kinetics of microbial sulfate reduction in estuarine sediments. Geochim. Cosmochim. Acta 70, 1148–1162. https://doi.org/10.1016/j. gca. 2005.11.002
- Pallud, C., Meile, C., Laverman, A.M., Abell, J., Van Cappellen, P., 2007. The use of flowthrough sediment reactors in biogeochemical kinetics: methodology and examples of

- applications. Mar. Chem. 106, 256–271. https://doi.org/10.1016/j.
- Parikh, S.J., Goyne, K.W., Margenot, A.J., Mukome, F.N.D., Calderón, F.J., 2014. Soil chemical insights provided through vibrational spectroscopy. Adv. Agron. 126, 1–148. https://doi.org/10.1016/B978-0-12-800132-5.00001-8.
- Pati, A., Gronow, S., Lapidus, A., Copeland, A., Glavina Del Rio, T., Nolan, M., Lucas, S., Tice, H., Cheng, J.-F., Han, C., Chertkov, O., Bruce, D., Tapia, R., Goodwin, L., Pitluck, S., Liolios, K., Ivanova, N., Mavromatis, K., Chen, A., Palaniappan, K., Land, M., Hauser, L., Chang, Y.-J., Jeffries, C.D., Detter, J.C., Rohde, M., Göker, M., Bristow, J., Eisen, J.A., Markowitz, V., Hugenholtz, P., Klenk, H.-P., Kyrpides, N.C., 2010. Complete genome sequence of Arcobacter nitrofigilis type strain (CIT). Stand Genomic Sci. 2, 300–308. https://doi.org/10.4056/sigs.912121.
- Poffenbarger, H.J., Needelman, B.A., Megonigal, J.P., 2011. Salinity influence on methane emissions from tidal Marshesg. Wetlands 31, 831–842. https://doi.org/ 10.1007/s13157-011-0197-0.
- Quast, C., Pruesse, E., Yilmaz, P., Gerken, J., Schweer, T., Yarza, P., Peplies, J., Glockner, F.O., 2012. The SILVA ribosomal RNA gene database project: improved data processing and web-based tools. Nucleic Acids Res. 41, D590–D596. https:// doi.org/10.1093/nar/gks1219.
- Shen, J., Liu, H., Zhou, H., Chen, R., 2022. Specific characteristics of the microbial community in the groundwater fluctuation zone. Environ. Sci. Pollut. Res. Int. 29, 76066–76077. https://doi.org/10.1007/s11356-022-21166-1.
- Singer, E., Emerson, D., Webb, E.A., Barco, R.A., Kuenen, J.G., Nelson, W.C., Chan, C.S., Comolli, L.R., Ferriera, S., Johnson, J., Heidelberg, J.F., Edwards, K.J., 2011. Mariprofundus ferrooxydans PV-1 the first genome of a marine Fe(II) oxidizing Zetaproteobacterium. PloS One 6, e25386. https://doi.org/10.1371/journal. pone.0025386.
- Smith, A.J., Noyce, G.L., Megonigal, J.P., Guntenspergen, G.R., Kirwan, M.L., 2022. Temperature optimum for marsh resilience and carbon accumulation revealed in a whole-ecosystem warming experiment. Glob. Chang. Biol. 28, 3236–3245. https://doi.org/10.1111/gcb.16149.
- Solorzano, L., 1969. Determination of ammonia in natural waters by phenolhypochlorite method. Limnol. Oceanogr. 14, 799–801.
- Spivak, A.C., Sanderman, J., Bowen, J.L., Canuel, E.A., Hopkinson, C.S., 2019. Global-change controls on soil-carbon accumulation and loss in coastal vegetated ecosystems. Nat. Geosci. 12, 685–692. https://doi.org/10.1038/s41561-019-0435-2.
- Sun, Y., Ding, A., Zhao, X., Chang, W., Ren, L., Zhao, Y., Song, Z., Hao, D., Liu, Y., Jin, N., Zhang, D., 2022. Response of soil microbial communities to petroleum hydrocarbons at a multi-contaminated industrial site in Lanzhou, China. Chemosphere 306, 135559. https://doi.org/10.1016/j.chemosphere.2022.135559.
- Tancsics, A., Szalay, A.R., Farkas, M., Benedek, T., Szoboszlay, S., Szabo, I., Lueders, T., 2018. Stable isotope probing of hypoxic toluene degradation at the Siklos aquifer reveals prominent role of Rhodocyclaceae. FEMS Microbiol. Ecol. 94, fiy088. https://doi.org/10.1093/femsec/fiy088.
- Thingstad, T.F., Øvreås, L., Vadstein, O., 2022. Mechanisms generating dichotomies in the life strategies of heterotrophic marine prokaryotes. Diversity 14, 217. https://doi.org/10.3390/d14030217.

- Thomas, F., Giblin, A.E., Cardon, Z.G., Sievert, S.M., 2014. Rhizosphere heterogeneity shapes abundance and activity of sulfur-oxidizing bacteria in vegetated salt marsh sediments. Front. Microbiol. 5, 309. https://doi.org/10.3389/fmicb.2014.00309.
- Treseder, K.K., Kivlin, S.N., Hawkes, C.V., 2011. Evolutionary trade-offs among decomposers determine responses to nitrogen enrichment. Ecol. Lett. 14, 933–938. https://doi.org/10.1111/j.1461-0248.2011.01650.x.
- Turner, R.E., 2011. Beneath the salt marsh canopy: loss of soil strength with increasing nutrient loads. Estuar. Coasts 34, 1084–1093. https://doi.org/10.1007/s12237-010-9341-v.
- Valiela, I., Teal, J.M., Sass, W.J., 1975. Production and dynamics of salt marsh vegetation and the effects of experimental treatment with sewage sludge. Biomass, Prod. Speies Compos. J. Appl. Ecol. 12, 973–981. https://doi.org/10.2307/2402103.
- Veum, K.S., Goyne, K.W., Kremer, R.J., Miles, R.J., Sudduth, K.A., 2013. Biological indicators of soil quality and soil organic matter characteristics in an agricultural management continuum. Biogeochemistry 117, 81–99. https://doi.org/10.1007/ s10533-013-9868-7.
- Vineis, J.H., Bulseco, A.N., Bowen, J.L., 2023. Microbial chemolithoautotrophs are abundant in salt marsh sediment following long-term experimental nitrate enrichment. FEMS Microbiol. Lett. 370, fnad082. https://doi.org/10.1093/femsle/fnad082
- Vizza, C., West, W.E., Jones, S.E., Hart, J.A., Lamberti, G.A., 2017. Regulators of coastal wetland methane production and responses to simulated global change. Biogeosciences 14, 431–446. https://doi.org/10.5194/bg-14-431-2017.
- Wang, F., Kroeger, K.D., Gonneea, M.E., Pohlman, J.W., Tang, J., 2019. Water salinity and inundation control soil carbon decomposition during salt marsh restoration: an incubation experiment. Ecol. Evol. 9, 1911–1921. https://doi.org/10.1002/ ecc3.4884.
- Warren, R.S., Fell, P.E., Rozsa, R., Brawley, A.H., Orsted, A.C., Olson, E.T., Swamy, V., Niering, W.A., 2002. Salt marsh restoration in Connecticut: 20 years of science and management. Restor. Ecol. 10, 497–513. https://doi.org/10.1046/j.1526-100X.2002.01031.x.
- Watson, E.B., Oczkowski, A.J., Wigand, C., Hanson, A.R., Davey, E.W., Crosby, S.C., Johnson, R.L., Andrews, H.M., 2014. Nutrient enrichment and precipitation changes do not enhance resiliency of salt marshes to sea level rise in the northeastern U.S. Clim. Change 125, 501–509. https://doi.org/10.1007/s10584-014-1189-x.
- Weston, N.B., Giblin, A.E., Banta, G.T., Hopkinson, C.S., Tucker, J., 2010. The effects of varying salinity on ammonium exchange in estuarine sediments of the Parker River, Massachusetts. Estuar. Coasts 33, 985–1003. https://doi.org/10.1007/s12237-010-9282-5
- Wigand, C., Brennan, P., Stolt, M., Holt, M., Ryba, S., 2009. Soil respiration rates in coastal marshes subject to increasing watershed nitrogen loads in southern New England, USA. Wetlands 29, 952–963. https://doi.org/10.1672/08-147.1.
- Yin, G., Hou, L., Liu, M., Liu, Z., Gardner, W.S., 2014. A novel membrane inlet mass spectrometer method to measure 15NH4+ for isotope-enrichment experiments in aquatic ecosystems. Environ. Sci. Technol. 48, 9555–9562. https://doi.org/10.1021/es501261s.
- Zedler, J.B., 2000. Progress in wetland restoration ecology. Trends Ecol. Evol. 15, 402–407. https://doi.org/10.1016/S0169-5347(00)01959-5.